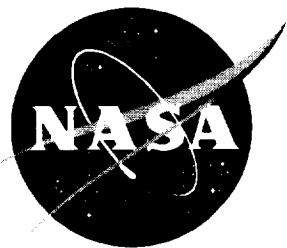


NASA Contractor Report 4574



Stopping Powers and Cross Sections Due to Two-Photon Processes in Relativistic Nucleus-Nucleus Collisions

*Wang K. Cheung and John W. Norbury
University of Wisconsin • La Crosse, Wisconsin*

National Aeronautics and Space Administration
Langley Research Center • Hampton, Virginia 23681-0001

Prepared for Langley Research Center
under Grant NAG1-1457

March 1994

List of Symbols

A_μ	photon field
\vec{B}	magnetic field
b	impact parameter between two nuclei
c	velocity of light
$-\frac{dE}{dx}$	stopping power
\vec{E}	electric field
e^+, e^-	positron, electron
$F(\omega_1, \omega_2)$	two-photon distribution function associated with photons of frequencies ω_1 and ω_2
\hat{f}	Fourier transform of a function f of one variable
$ f\rangle$	final state
G_F	Fermi coupling constant
h_f	coupling between Higgs and fermion
$ i\rangle$	initial state
$K_0(x), K_1(x)$	modified Bessel functions of order 0 and 1
k_i	momentum of a photon
L	two-photon luminosity function
\mathcal{L}_{int}	interaction lagrangian
$\mathcal{L}_{\text{int}}^{(e)}$	interaction lagrangian for coupling between a fermion field and the photon field
$\mathcal{L}_{\text{int}}^{(h)}$	interaction lagrangian for coupling between a fermion field and a Higgs field
l^+, l^-	charged leptons

m	mass
m_e	mass of electron
m_f	mass of a fermion
m_l	mass of lepton
$N(\omega, b)$	photon frequency distribution at frequency ω and distance b from the nucleus emitting the photons
$n(\omega, b)$	number of photons per unit frequency interval per unit area at frequency ω and distance b from the nucleus emitting the photons
$P(b)$	probability for producing a particle pair when two nuclei collide at impact parameter b
p_h	momentum of a Higgs particle
p_-, p_+	momenta of charged particles
q_f	fermion charge
S	S -matrix
$S^{(n)}$	n -th order term of S -matrix
\vec{S}	Poynting vector
s^+, s^-	charged scalars
s_-, s_+	polarizations of charged leptons
T	time ordering
T_0	normalization time
$\bar{u}(p_-, s_-), v(p_+, s_+)$	lepton and anti-lepton spinors associated with momenta p_-, p_+ and polarizations s_-, s_+
v	velocity
V^+, V^-	charged vectors

W	mass of produced system of particle(s)
W^+, W^-	charged W -bosons
H^0	neutral Higgs scalar
Z	nucleus with charge Z
α	fine structure constant
Γ	width of a particle
γ	$(1 - v^2/c^2)^{-1/2}$, Lorentz factor associated with velocity v
γ_μ	Dirac γ matrices
ϵ_i	photon polarization
Λ_i	mass of photon
ρ	number of nuclei per unit volume
σ	cross section
$\sigma_{\gamma\gamma}(\omega_1, \omega_2)$	photon-photon cross section associated with photons of frequencies ω_1 and ω_2
$\psi(x)$	lepton field operator
Ω	normalization volume
ω	frequency of photon

1. Introduction

The radiation dose received from high energy galactic cosmic rays (GCR) is a limiting factor in the design of long duration space flights and the building of lunar and martians habitats. It is of vital importance to have an accurate understanding of the interactions of GCR in order to assess the radiation environment that astronauts will be exposed to.

Most previous studies have concentrated on strong interaction processes in GCR. However there are also very large effects due to electromagnetic (EM) interactions. EM studies have previously concentrated on single photon exchange leading to nucleon removal. However two-photon processes also occur which lead to the production of lepton pairs with cross sections of the order of *kilobarns*. Also at high energy the stopping powers from these processes can exceed that due to atomic collisions. Thus even though very high energy GCR are not as abundant as lower energy GCR they still must be considered due to the fact that the cross sections and stopping powers are so much larger than normal.

In this report we describe our first efforts at understanding these EM production processes due to two-photon collisions. More specifically, we shall consider particle production processes in relativistic heavy ion collisions through two-photon exchange. Examples of this broad category of processes include:

$$Z_1 Z_2 \rightarrow Z_1 Z_2 l^+ l^- \quad (1.1a)$$

$$Z_1 Z_2 \rightarrow Z_1 Z_2 s^+ s^- \quad (1.1b)$$

$$Z_1 Z_2 \rightarrow Z_1 Z_2 V^+ V^- \quad (1.1c)$$

$$Z_1 Z_2 \rightarrow Z_1 Z_2 H^0 \quad (1.1d)$$

in which $l^+ l^-$ denote charged leptons, $s^+ s^-$ denote charged scalars, $V^+ V^-$ denote charged vector particles, and H^0 is a neutral Higgs scalar.

We shall limit our consideration to cases in which the colliding nuclei are identical, so that $Z_1 = Z_2 = Z$. An important Feynman diagram that contributes to (1.1a), (1.1b), and (1.1c) is shown in the following figure (fig. 1).

For process (1.1d), an important diagram is shown in figure 2, in which the triangular loop receives contributions from quarks, leptons and W gauge bosons.

These processes are important for the following reasons (ref. 1).

- (1) These kinds of processes become increasingly important as the energy of the colliding nuclei increases, since their cross sections increase with energy. Thus their contributions to the stopping power of high energy ions also become more important at high energies.
- (2) These processes can be channels for production of charged particles, e.g., l^+l^- , W^+W^- , and neutral particles such as Higgs bosons, and various mesons.
- (3) For high Z nuclei these processes can be used for studying non-perturbative effects in the electromagnetic interaction.
- (4) They must be taken into account in the study of strong interaction effects in heavy ion collisions since they can lead to important background events, and must be taken into account also in the design of experimental set up, since they can lead to significant beam loss.

Section 2 of this report gives a brief survey of a few major approaches used in the calculations for these processes. Section 3 examines some results of our calculations. We then point out briefly some open questions and make a few concluding remarks in Section 4.

The purpose of this report is threefold. (1) It gives a simple, elementary introduction to this field. (2) It provides sample calculations for illustrating the approach we use. (3) The background and techniques developed here can be used as a general base for launching further and more specialized studies into this field.

While it is not our main goal here to obtain new and original results, some of our results are possibly new, and are as yet not available in the literature.

2. A Brief Survey of Different Approaches

In this section, we briefly list a few major approaches used in calculating cross sections for the kind of processes we are interested in. The first approach has been discussed in

references 2 and 3. In this approach, each colliding nucleus is replaced by an equivalent spectrum of photons. Each nucleus is considered to move in a straight line, unperturbed by the interaction. At a distance b from the line of motion of a nucleus, a spectrum of photons is generated, whose frequency distribution has the form:

$$N(\omega, b) = \frac{Z^2 \alpha}{\pi^2} \left(\frac{\omega}{\gamma v} \right)^2 \left(\frac{c}{v} \right)^2 \left[K_1^2(x) + \frac{1}{\gamma^2} K_0^2(x) \right] \quad (2.1a)$$

where

$$x \equiv \frac{\omega b}{\gamma v} \quad (2.1b)$$

K_0 , K_1 are modified Bessel functions, see reference 4, Sections 3.7 and 15.4.

The cross section for this process can be written as an integral of a photon distribution function multiplied by a photon-photon cross section.

$$\sigma = \int \frac{d\omega_1}{\omega_1} \int \frac{d\omega_2}{\omega_2} F(\omega_1, \omega_2) \sigma_{\gamma\gamma}(\omega_1, \omega_2), \quad (2.3a)$$

where

$$F(\omega_1, \omega_2) = 2\pi \int_{b_{1\min}}^{\infty} b_1 db_1 \int_{b_{2\min}}^{\infty} b_2 db_2 \int_0^{2\pi} d\phi N(\omega_1, b_1) \times N(\omega_2, b_2) \theta(b' - R_1 - R_2) \quad (2.2b)$$

and

$$b' = \left(b_1^2 + b_2^2 - 2b_1 b_2 \cos \phi \right)^{1/2} \quad (2.2c)$$

where ω_1 and ω_2 are the frequencies of the photons emitted by the nuclei, b_1 and b_2 are the distances of the nuclei from the point where the photons collide. Details can be found in Appendix A. Various differential cross sections can be derived from these equations. First we consider $\frac{d\sigma}{dW^2}$ where W is the mass of the produced charged particle pair. We note that $W^2 = 4\omega_1\omega_2$. Hence we can equate in (2.2a)

$$\sigma = \int \frac{d\omega_1}{\omega_1} \int \frac{dW^2}{W^2} F \left(\omega_1, \frac{W^2}{4\omega_1} \right) \sigma_{\gamma\gamma} \left(\omega_1, \frac{W^2}{4\omega_1} \right), \quad (2.3a)$$

and

$$\frac{d\sigma}{dW^2} = \frac{1}{W^2} \int \frac{d\omega_1}{\omega_1} F\left(\omega_1, \frac{W^2}{4\omega_1}\right) \sigma_{\gamma\gamma}\left(\omega_1, \frac{W^2}{4\omega_1}\right). \quad (2.3b)$$

Next we define the probability for producing a particle pair $P(b)$ at impact parameter b by

$$P(b) \equiv \frac{1}{2\pi b} \frac{d\sigma}{db} \quad (2.4a)$$

where

$$\frac{d\sigma}{db} = \int \frac{d\omega_1}{\omega_1} \int \frac{d\omega_2}{\omega_2} F(\omega_1, \omega_2) \sigma_{\gamma\gamma}(\omega_1, \omega_2) \delta(b - b'), \quad (2.4b)$$

in which it is understood that the δ function is to be taken inside the triple integral which defines $F(\omega_1, \omega_2)$. The correctness of (2.4) can be checked by integrating both sides of (2.4b) over all values of the impact parameter b , which then yields (2.3a) for the total cross section. $P(b)$ is the probability for the events in which two nuclei collide with each other at impact parameter b , producing a charged particle pair in the process. A quantity L , known as the two-photon luminosity function is defined by (see ref. 2, eqs. (1), (9), and (10))

$$L = \int \frac{d\omega_1}{\omega_1} \int \frac{dW^2}{W^2} F\left(\omega_1, \frac{W^2}{4\omega_1}\right). \quad (2.5a)$$

So

$$\frac{dL}{dW^2} = \frac{1}{W^2} \int \frac{d\omega_1}{\omega_1} F\left(\omega_1, \frac{W^2}{4\omega_1}\right), \quad (2.5b)$$

and

$$\frac{d\sigma}{dW^2} = \frac{dL}{dW^2} \sigma_{\gamma\gamma}(W^2), \quad (2.5c)$$

where we have used the fact that $\sigma_{\gamma\gamma}(\omega_1, \omega_2)$ actually depends only on W^2 so that we can write

$$\sigma_{\gamma\gamma}(\omega_1, \omega_2) = \sigma_{\gamma\gamma}(W^2). \quad (2.6)$$

It is our view that equation (10) of reference 2 is in error, and have duly corrected the error in the above definition of the luminosity function L . For the stopping power calculation, we use the formula

$$-\frac{dE}{dx} = \rho \int \frac{d\omega_1}{\omega_1} \int \frac{d\omega_2}{\omega_2} (\omega_1 + \omega_2) F(\omega_1, \omega_2) \sigma_{\gamma\gamma}(\omega_1, \omega_2), \quad (2.7)$$

where ρ is the number of nuclei per unit volume.

The second type of approach has been applied to a related set of purely quantum electrodynamic (QED) processes: $e^+e^- \rightarrow e^+e^-l^+l^-$. This process can be calculated within the framework of QED. Cross sections can be obtained numerically by Monte-Carlo integration. Approximate formulas for total cross sections have also been obtained. See references 5 and 6. This kind of approach can be modified to apply to relativistic nucleus-nucleus collisions, provided one takes into account properly the effects of nuclear currents. See reference 7, Section II.

In an approach closely related to this second type of approach, Bottcher and Strayer treated the colliding nuclei classically, by regarding them as classical charge distributions. The remaining amplitude for the production of charged particle pair is then obtained in the framework of QED. Thus for the case of the reaction $Z_1Z_2 \rightarrow Z_1Z_2l^+l^-$ the total cross section can be written in the form (ref. 8, eq. (10), p. 38):

$$\begin{aligned} \sigma = & \frac{Z_1^2 Z_2^2}{4v^2} (4\pi\alpha)^4 \int \frac{d^3p_- d^3p_+ d^2k_{1\perp}}{(2\pi)^8 2p_{-0} 2p_{+0}} f_1^2(k_1^2) f_2^2(k_2^2) \\ & \times \sum_{s_-, s_+} \left| \bar{u}(p_-, s_-) \left[\not{\epsilon}_1 \frac{1}{\not{p}_- - \not{k}_1 - m_l} \not{\epsilon}_2 \right. \right. \\ & \left. \left. + \not{\epsilon}_2 \frac{1}{\not{p}_- - \not{k}_2 - m_l} \not{\epsilon}_1 \right] v(p_+, s_+) \right|^2, \end{aligned} \quad (2.8)$$

where v denotes the velocity of one of the nuclei in the center of momentum frame, p_- and p_+ are the momenta of the produced leptons, s_- and s_+ are their polarizations, $\bar{u}(p_-, s_-)$ and $v(p_+, s_+)$ are the lepton spinors, k_1 and k_2 are the momenta of the exchanged photons, and f_1 and f_2 are the nuclear form factors. For any 4-vector A , the slash notation \not{A} is defined by

$$\not{A} = \sum_{\mu=0}^3 A_\mu \gamma^\mu, \quad (2.9)$$

where γ^μ are the Dirac γ -matrices. See for instance reference 9, Appendix 2, pages 355–361.

3. Results

In this report, we adopt the approach discussed in references 2 and 3. As samples of our calculations, we present a number of results for the process $^{208}\text{Pb}^{208}\text{Pb} \rightarrow ^{208}\text{Pb}^{208}\text{Pb} l^+l^-$, and some others. Most of our calculations are done for colliding beam energies of 3400 Gev and 8000 Gev per nucleon. The impact parameter b varies over the range from 10 fm to 1000 fm. The mass of l^+l^- varies from a threshold equal to $2m_l$ up to about 1000 Gev. In Appendix B we list the photon-photon cross sections for the following processes:

$$\gamma\gamma \rightarrow l^+l^- \quad (3.1a)$$

$$\gamma\gamma \rightarrow s^+s^- \quad (3.1b)$$

$$\gamma\gamma \rightarrow V^+V^- \quad (3.1c)$$

$$\gamma\gamma \rightarrow H^0 \quad (3.1d)$$

The derivations of some of these cross sections are also given there. By using (2.2)–(2.6), we can then obtain various luminosity functions, differential and total cross sections, probabilities, and stopping powers.

Table 1 shows the total cross section for $ZZ \rightarrow ZZe^+e^-$. We compare our numerical results based on (2.1) and (2.2), with the results based on the Racah formula (ref. 5, eq. (F.1), p. 276)

$$\sigma = \frac{28 (Z_1 Z_2 \alpha^2)^2}{27\pi m_e^2} (l^3 - Al^2 + Bl + C) \quad (3.2)$$

where

$$A \approx 6.36, \quad B \approx 15.7, \quad C \approx -13.8,$$

$$l = \ln \left(\frac{2p_1 \cdot p_2}{m_1 m_2} \right) = \ln (2\gamma_p).$$

Z_i , p_i , and m_i , $i = 1, 2$ are the charges, momenta, and masses of the colliding nuclei.

Table 1

Colliding nuclei Z	Incident energy/nucleon E (GeV)	Total cross section (kilobarn)	
		Our results	Calculated from formula
O-16	3400.0	0.2241×10^{-1}	0.2216×10^{-1}
	8000.0	0.3052×10^{-1}	0.3020×10^{-1}
Al-27	3400.0	0.1563	0.1545
	8000.0	0.2128	0.2106
Fe-56	3400.0	0.2500×10^1	0.2473×10^1
	8000.0	0.3404×10^1	0.3370×10^1
Pb-208	3400.0	0.2473×10^3	0.2445×10^3
	8000.0	0.3366×10^3	0.3333×10^3

Table 2 shows the corresponding stopping power calculations. The energies of the incident particles are given for both the case of colliding beams and also the case of an incident beam colliding with a fixed target.

Table 2

Incident energy/nucleon E (Gev, colliding beams)	Incident energy/nucleon E (Gev, fixed target)	$\frac{1}{\rho} \times \left(-\frac{dE}{dx}\right)$ (Gev fm ²)	$\left(-\frac{dE}{dx}\right)$ (Mev/cm)
0.9636	1.039	0.2129×10^{-2}	7.02×10^{-4}
0.1367×10^1	3.036	0.4585×10^2	1.51×10^1
0.2704×10^1	14.64	0.6909×10^3	2.28×10^2
3400.0	0.2462×10^8	0.2032×10^{11}	6.70×10^9
8000.0	0.1363×10^9	0.1182×10^{12}	3.90×10^{10}
For Pb-208, $\rho \approx 3.30 \times 10^{22}$ cm ⁻³			

Note that the stopping power for e^+e^- production increases with energy. So as the energy of the colliding nuclei increases, the contribution of this process to stopping power also becomes more important. In contrast, the contribution to stopping power from atomic collision and other processes first increases with energy, and then decreases. Hence, as energy increases, eventually these other contributions become less important. To put our results into perspective, we note that for Fe-56 at a kinetic energy of 1 Gev, its stopping power in water due to atomic collision is around 10^4 Mev/cm, see reference 10, figure 2.15, p. 74.

In figure 3, we give plots of $W^2 \frac{dL}{dW^2}$ as a function of W in different ranges of W . The differential cross section $\frac{d\sigma}{dW^2}$ can be obtained from $\frac{dL}{dW^2}$ by multiplying $\frac{dL}{dW^2}$ by a $\gamma\gamma$ cross section as in (2.5c).

Figures 4a-d show plots of $\sigma_{\gamma\gamma}(W^2)$ for the reactions $\gamma\gamma \rightarrow l^+l^-$, $\gamma\gamma \rightarrow s^+s^-$, $\gamma\gamma \rightarrow V^+V^-$, and $\gamma\gamma \rightarrow H^0$.

Figure 5 shows plots of $P(b)$ for the reaction $^{208}\text{Pb}^{208}\text{Pb} \rightarrow ^{208}\text{Pb}^{208}\text{Pb} e^+e^-$ at different energies.

Figure 6 presents plots of the total cross section for the process $^{208}\text{Pb}^{208}\text{Pb} \rightarrow ^{208}\text{Pb}^{208}\text{Pb} H^0$.

We have compared some of our results with the published results of Papageorgiu and Baur, and found good agreement. In the following, we give a sample of such comparisons.

Table 3

	W (Gev)	W/\sqrt{s}	$W^2 \frac{dL}{dW^2}$	
			Our result	Papageorgiu's result
Incident energy/ nucleon (colliding beams) E = 3400.0 Gev	100.0	0.7070×10^{-4}	0.3152×10^3	0.33×10^3
	141.4	0.1000×10^{-4}	0.8630×10^2	0.90×10^2
	212.2	0.1500×10^{-3}	0.1206×10^2	0.13×10^2
	282.9	0.2000×10^{-3}	0.1990×10^1	0.21×10^1
E = 8000.0 Gev	19.0	0.5709×10^{-4}	0.6129×10^3	0.70×10^3
	280.0	0.8413×10^{-4}	0.1708×10^3	0.20×10^3
	370.0	0.1112×10^{-3}	0.5444×10^2	0.60×10^2
	460.0	0.1382×10^{-3}	0.1881×10^2	0.20×10^2
	550.0	0.1653×10^{-3}	0.6866×10^1	0.70×10^1
	640.0	0.1923×10^{-3}	0.2606×10^1	0.28×10^1

Table 4

Incident energy/nucleon (colliding beams) $E = 3755.6 \text{ Gev}$		
W(Gev)	$\frac{d\sigma}{dW^2} (\text{fm}^2 \text{ Gev}^{-2})$	
	Our result	Baur's result
0.1200×10^{-2}	0.6188×10^{13}	0.62×10^{13}
0.1414×10^{-2}	0.4923×10^{13}	0.48×10^{13}
0.1732×10^{-2}	0.2777×10^{13}	0.28×10^{13}
0.2000×10^{-2}	0.1714×10^{13}	0.17×10^{13}
0.2200×10^{-2}	0.1222×10^{13}	0.12×10^{13}
0.2400×10^{-2}	0.8894×10^{12}	0.92×10^{12}
0.2600×10^{-2}	0.6607×10^{12}	0.69×10^{12}
0.3000×10^{-2}	0.3846×10^{12}	0.40×10^{12}

Papageorgiu and Baur's results were taken from appropriate graphs in their papers (ref. 2, fig. 3; and ref. 3, fig. 9).

Cross sections are expected to scale roughly as $Z_1^2 Z_2^2$. For our case $Z_1 = Z_2 = Z$. So in order to obtain the corresponding cross sections, luminosity function, or stopping power for different nuclei, one can simply multiply the results we have here by a factor $\frac{Z_1^2 Z_2^2}{(Z=82)^4}$. Thus if one wants the results for $Al Fe$ collision, one can multiply the results presented in this section by the conversion factor $\frac{13^2 56^2}{82^4}$. The different nuclear sizes are expected to affect the results also. However for a rough order of magnitude estimate, such a simple scaling is expected to be reasonably accurate.

4. Open Questions and Conclusions

For small values of b , and m_l , such as $m_l = m_e$, $P(b)$ exceeds 1. This signifies the breakdown of perturbation theory. The question as to how to extract meaningful results from theory is under active investigation. See reference 11. In our simple approach, we have regarded the nuclei as point charges. By using form factors for the nuclei, the problem of violation of unitarity is expected to be somewhat ameliorated. However this problem still needs to be addressed, because for high Z nuclei, the coupling constant for the electromagnetic interaction is of the order Ze , even with nuclear form factor taken into account, which may therefore still lead to a breakdown of the perturbative approach to cross-section calculation. In a collaboration with Mirek Fatyga of Brookhaven National Laboratory (BNL), we shall investigate lepton pair production and neutral meson production (such as ϵ^0 , η^0) in high energy heavy ion collisions. In these processes, we shall look for possible deviation in the measured rates or cross sections from values calculated by perturbation theory.

In many studies of the type of processes considered here, various approximations are used. We have mentioned the equivalent photon approximation, and the semi-classical approximation. Also, in the approach of references 2 and 3, which we have adopted in this report, the effect due to phase coherence of the electromagnetic field generated by the nuclei has not been properly taken into account. One needs to investigate how valid these approximations are and what the regions of validity are for them.

When one is primarily interested in the kind of electromagnetic processes discussed here, one needs to be able to estimate reliably the background due to strong interaction. Furthermore, there are other electromagnetic processes that also need to be studied, in addition to the ones we have looked at, even though the ones we have considered are among the most important.

In summary, we have given a brief introduction to two-photon exchange processes in high energy heavy ion collisions. Our calculations are based on an approach discussed in

references 2 and 3. In view of the significance of this class of processes, and the many open questions that remain to be answered, we believe that further study in these areas will be valuable, not only for gaining a better understanding into these processes themselves, but also for studies and experiments in strong interaction physics.

In the following Appendices, we discuss the derivation of some of the formulas we have used. We look at the equivalent photon approximation in Appendix A and show how this is applied to the two-photon exchange processes in relativistic nucleus-nucleus collisions. Then in Appendix B, derivations are given for some $\gamma\gamma$ cross sections. Appendix C provides a derivation of the fermion contribution to the process $H^0 \rightarrow \gamma\gamma$. In Appendix D, we look at the details of how certain integrals encountered in our calculations are evaluated. Finally Appendix E gives a simple derivation of the formula (2.7) used for calculating stopping power.

Appendix A. Equivalent Photon Approximation

Consider a charge q moving along the x -axis. The effect of this charge on another charge located a distance b from the x -axis can be approximately calculated as follows.

By first considering the electromagnetic (EM) field due to q in its own rest frame, and then making a Lorentz transformation to the laboratory frame, it is straight forward to show that the electromagnetic field due to q is given by

$$E_1 = -qv\gamma t(b^2 + \gamma^2 v^2 t^2)^{-3/2} \quad (\text{A.1a})$$

$$E_2 = qb\gamma(b^2 + \gamma^2 v^2 t^2)^{-3/2} \quad (\text{A.1b})$$

$$B_3 = \frac{v}{c} E_2 = q \frac{v}{c} b\gamma(b^2 + \gamma^2 v^2 t^2)^{-3/2} \quad (\text{A.1c})$$

$$E_3 = B_1 = B_2 = 0 \quad (\text{A.1d})$$

$t = 0$ corresponds to the instant when q passes through the origin. When $v \approx c$, the components E_2 and B_3 can be thought of as the components of a pulse of plane-polarized EM wave travelling along x . The energy flux of this EM field is given by the Poynting vector

$$\vec{S} = \frac{c}{4\pi} \vec{E} \times \vec{B}. \quad (\text{A.2})$$

So ignoring E_1 for the moment, \vec{S} points along x , and its magnitude is

$$|\vec{S}| = \frac{c}{4\pi} E_2^2, \quad (\text{A.3})$$

in which we have made the approximation $\frac{v}{c} \approx 1$. Over a unit area, the flow of energy is

$$\int_{-\infty}^{\infty} |\vec{S}| dt = \frac{c}{4\pi} \int_{-\infty}^{\infty} E_2^2(t) dt. \quad (\text{A.4a})$$

Using Parseval's theorem, we therefore have

$$\int_{-\infty}^{\infty} |\vec{S}| dt = \frac{c}{4\pi} \int_{-\infty}^{\infty} |\hat{E}_2(\omega)|^2 d\omega, \quad (\text{A.4b})$$

where \hat{E}_2 is the Fourier transform (FT) of E_2 , defined by

$$\hat{f}(\omega) \equiv \frac{1}{\sqrt{2\pi}} \int_{-\infty}^{\infty} f(t) e^{-i\omega t} dt \quad (\text{A.5})$$

Hence the quantity $\hat{S}_2(\omega)$, defined by

$$\hat{S}_2(\omega) = \frac{c}{4\pi} |\hat{E}_2(\omega)|^2, \quad (\text{A.6})$$

can be thought of as the energy per unit frequency per unit area of the EM field at frequency ω generated by the moving charge q . To obtain the photon number per unit frequency per unit area at frequency ω , we set $n_2(\omega) = \frac{1}{\hbar\omega} \hat{S}_2(\omega)$, since each photon has energy $\hbar\omega$. For the function $n_2(\omega)$, the dependence on the distance b is implicit. To make the dependence on b explicit, we can write instead

$$n_2(\omega, b) = \frac{1}{\hbar\omega} \hat{S}_2(\omega). \quad (\text{A.7})$$

From (A.1b), we obtain

$$\hat{E}_2(\omega) = \frac{q}{bv} \sqrt{\frac{2}{\pi}} \frac{\omega b}{\gamma v} K_1\left(\frac{\omega b}{\gamma v}\right) \quad (\text{A.8})$$

Hence

$$\hat{S}_2(\omega) = \frac{c}{4\pi} \frac{2}{\pi v^2} \left(\frac{q}{b}\right)^2 \left(\frac{\omega b}{\gamma v}\right)^2 K_1^2\left(\frac{\omega b}{\gamma v}\right) \quad (\text{A.9})$$

The remaining component E_1 , of the EM field can be complemented by a magnetic field so that they can be considered to form a pulse of plane polarized EM wave. The same treatment can be applied to these components, so that the energy spectrum can be similarly obtained as before. The result is

$$\begin{aligned} \hat{S}_1(\omega) &= \frac{c}{4\pi} |\hat{E}_1(\omega)|^2 = \frac{c}{4\pi} \frac{1}{\gamma^2} \frac{1}{v^2} \left(\frac{q}{b}\right)^2 \frac{2}{\pi} \left(\frac{\omega b}{\gamma v}\right)^2 \\ &\quad \times K_0^2\left(\frac{\omega b}{\gamma v}\right) \end{aligned} \quad (\text{A.10})$$

The effect of this pulse is roughly $\frac{1}{\gamma^2}$ that of the first pulse. So at high velocity, the second pulse can be neglected when compared with the first pulse.

In conventional treatment, the two pulses are simply added together, so that the effect due to the original moving charge q is replaced by a spectrum of photons whose number density is simply the sum of the number densities from the two pulses discussed above. Thus

one set

$$n(\omega, b) = \frac{1}{\hbar\omega} \left[\hat{S}_2(\omega) + \hat{S}_1(\omega) \right] = \frac{1}{\hbar\omega} \frac{c}{4\pi} \frac{1}{v^2} \left(\frac{q}{b} \right)^2 \frac{2}{\pi} \left(\frac{\omega b}{\gamma v} \right)^2 \times \left[K_1^2 \left(\frac{\omega b}{\gamma v} \right) + \frac{1}{\gamma^2} K_o^2 \left(\frac{\omega b}{\gamma v} \right) \right] \quad (\text{A.11})$$

After identifying $q = Ze$, $\frac{e^2}{\hbar c} = \alpha$, and noting

$$\hat{S}_i(-\omega) = \hat{S}_i(\omega) \quad \text{for } i = 1, 2, \quad (\text{A.12})$$

the photon energy spectrum

$$\begin{aligned} N(\omega, b) &= \hat{S}_1(\omega) + \hat{S}_2(\omega) + \hat{S}_1(-\omega) + \hat{S}_2(-\omega) \\ &= \frac{Z^2 e^2}{\pi^2} \frac{1}{c} \left(\frac{c}{v} \right)^2 \left(\frac{\omega}{\gamma v} \right)^2 \left[K_1^2 \left(\frac{\omega b}{\gamma v} \right) + \frac{1}{\gamma^2} K_o^2 \left(\frac{\omega b}{\gamma v} \right) \right] \\ &= \hbar \frac{Z^2 \alpha}{\pi^2} \left(\frac{c}{v} \right)^2 \left(\frac{\omega}{\gamma v} \right)^2 \left[K_1^2 \left(\frac{\omega b}{\gamma v} \right) + \frac{1}{\gamma^2} K_o^2 \left(\frac{\omega b}{\gamma v} \right) \right] \end{aligned} \quad (\text{A.13})$$

Application of the Equivalent Photon Approximation to Two-Photon Exchange Processes

When two nuclei Z_1 and Z_2 collide with each other, their EM interactions can be studied in terms of the EM interaction of the spectra of photons emitted by the nuclei. The situation can be pictured as in figure A.2.

The two photons γ_1 and γ_2 are considered as colliding head-on with each other. Taking a cross-sectional view perpendicular to the direction of motion of the nuclei, the situation can be pictured as shown in figure A.3.

From our previous discussion, the number of photons emitted by Z_1 at P , whose frequencies are between ω_1 and $\omega_1 + d\omega_1$, is $n(\omega_1, b_1) d\omega_1 b_1 db_1 d\phi_1$, where $n(\omega_1, b_1)$ is defined by (A.11). Similarly, the number of photons incident at P emitted by Z_2 is $n(\omega_2, b_2) d\omega_2 b_2 db_2 d\phi_2$. Therefore the EM cross section for the collision of Z_1 and Z_2 through two-photon exchange can be written as

$$\begin{aligned} \sigma &= \int n(\omega_1, b_1) n(\omega_2, b_2) \sigma_{\gamma\gamma}(\omega_1, \omega_2) b_1 db_1 d\phi_1 b_2 db_2 d\phi_2 \\ &\quad \times \theta(b - R_1 - R_2) d\omega_1 d\omega_2 \end{aligned} \quad (\text{A.14})$$

in which R_1 and R_2 stand for the nuclear radii of Z_1 and Z_2 , and the θ -function takes into account that when $b < R_1 + R_2$, the two nuclei overlap, and the EM interaction is swamped by the strong interaction of the nuclei, and so one needs to restrict b to values $> R_1 + R_2$ if one wants to look only at EM interactions.

Since $b = (b_1^2 + b_2^2 - 2b_1b_2 \cos \phi)^{1/2}$, the integration $\int d\phi_1 d\phi_2$ in (A.14) can be simplified if one integrates over ϕ_1 and converts the integration over ϕ_2 into an integration over ϕ :

$$\int d\phi_1 d\phi_2 \rightarrow 2\pi \int d\phi \quad (\text{A.15})$$

So (A.14) can be rewritten as

$$\begin{aligned} \sigma = 2\pi \int n(\omega_1, b_1) n(\omega_2, b_2) \sigma_{\gamma\gamma}(\omega_1, \omega_2) \theta(b - R_1 - R_2) \\ \times b_1 db_1 b_2 db_2 d\phi d\omega_1 d\omega_2. \end{aligned} \quad (\text{A.16})$$

If one now substitutes for $n(\omega_i, b_i)$, $i = 1, 2$, using (A.11), one obtains (2.2).

Concerning the cutoff for b_1 and b_2 , we observe the following. (A.14) involves an approximation, which consists of replacing the virtual photons emitted by Z_1 and Z_2 with real photons γ_1 and γ_2 . This approximation is valid only if the masses of the virtual photons Λ_1 and Λ_2 are small compared to the mass of the produced system W . (See ref. 5, Sections 6.1 and 6.7). By the uncertainty relations, $\Lambda_i \approx \frac{1}{b_i}$, $i = 1, 2$. Hence in order for the approximation in (A.13) to be valid, we must have $\Lambda_i < W$, or $\frac{1}{b_i} \lesssim W$. Therefore,

$$b_i \gtrsim \frac{1}{W} \quad (\text{A.17})$$

If b_i does not satisfy (A.17), the contribution to the cross section is small, and is generally considered negligible. See reference 5, Sections 6.1 and 6.2, and reference 12, Sections 7, 7.1–7.3. Another consideration for the values of b_i is that since we are interested in the effects of each nucleus acting as a single entity rather than as a collection of nucleons acting independently of each other, i.e., we are interested in the coherent effects of the collection of nucleons, we need to restrict

$$b_i > R_i. \quad (\text{A.18})$$

So for reactions in which the Compton wavelength of the produced system is smaller than the nuclear radii, i.e., $\frac{2}{W} < R_i$, we can set the minimum of b_i by

$$b_{i\min} = R_i. \quad (\text{A.19})$$

This is the case for $\mu^+\mu^-$ and $\tau^+\tau^-$ pair function. But for e^+e^- pair production, the Compton wavelength of an electron $\frac{1}{m_e}$ is $>R_i$. So we set the minimum of b_i by

$$b_{i\min} = \frac{2}{W}. \quad (\text{A.20})$$

Hence in general we set

$$b_{i\min} = \max \left\{ R_i, \frac{2}{W} \right\}$$

Note that when $W = 2m_e$ in (A.20), $b_{i\min} = \frac{1}{m_e}$, which is the cut off generally accepted in the literature for e^+e^- pair production (see e.g., reference 3, Section 3). With $b_{i\min}$ defined by (A.19) and (A.20), our calculations for e^+e^- pair production show good agreement with the results from the approximate formula (3.2), as is shown in Table 1.

Appendix B

First we list the cross sections for the processes in (3.1): $\gamma\gamma \rightarrow l^+l^-$, $\gamma\gamma \rightarrow s^+s^-$, $\gamma\gamma \rightarrow V^+V^-$, and $\gamma\gamma \rightarrow H^0$. (See ref. 2, eqs. (14)–(17), pp. 159, 160; and ref. 13, eqs. (10), (11), p. 95.)

$$\sigma(\gamma\gamma \rightarrow l^+l^-) = \frac{4\pi\alpha^2}{W^2} \left[2(1 + y_l - \frac{1}{2}y_l^2) \ln \left(\frac{1}{\sqrt{y_l}} + \sqrt{\frac{1}{y_l} - 1} \right) - (1 + y_l)\sqrt{1 - y_l} \right], \quad (\text{B.1a})$$

$$\sigma(\gamma\gamma \rightarrow s^+s^-) = \frac{2\pi\alpha^2}{W^2} \left[(1 + y_s)\sqrt{1 - y_s} - 2y_s \left(1 - \frac{1}{2}y_s \right) \ln \left(\frac{1}{\sqrt{y_s}} + \sqrt{\frac{1}{y_s} - 1} \right) \right], \quad (\text{B.1b})$$

$$\sigma(\gamma\gamma \rightarrow V^+V^-) = \frac{8\pi\alpha^2}{W^2} \left[\frac{1}{t_v} \left(1 + \frac{3}{4}t_v + 3t_v^2 \right) \Lambda - 3t_v(1 - 2t_v) \ln \left(\frac{1 + \Lambda}{1 - \Lambda} \right) \right], \quad (\text{B.1c})$$

where

$$y_l = \frac{4m_l^2}{W^2}, \quad y_s = \frac{4m_s^2}{W^2}, \quad (\text{B.2a})$$

$$t_v = \frac{m_v^2}{W^2}, \quad \Lambda = \sqrt{1 - 4t_v}. \quad (\text{B.2b})$$

W is the total energy of the two photons in the center of momentum frame.

$$\sigma(\gamma\gamma \rightarrow H^0) = \frac{8\pi^2}{m_H} \Gamma \delta(W^2 - m_H^2) \quad (\text{B.3})$$

where Γ can be written as (ref. 12, eq. (10), p. 95)

$$\Gamma = \frac{\alpha^2 G_F m_H^3}{8\pi^3 \sqrt{2}} |I|^2, \quad (\text{B.4})$$

and I in turn has the form (ref. 13, eqn. (11), p. 95)

$$I = \sum_q q^2 I_q + \sum_l I_l + I_w, \quad (\text{B.5a})$$

$$I_q = 3 [2\lambda_q + \lambda_q(4\lambda_q - 1)f(\lambda_q)], \quad (\text{B.5b})$$

$$I_l = 2\lambda_l + \lambda_l(4\lambda_l - 1)f(\lambda_l), \quad (\text{B.5c})$$

$$I_W = 3\lambda_W(1 - 2\lambda_W)f(\lambda_W) - 3\lambda_W - \frac{1}{2}, \quad (\text{B.5d})$$

where for $\lambda > \frac{1}{4}$

$$f(\lambda) = -2 \left(\arcsin \frac{1}{2\sqrt{\lambda}} \right)^2, \quad (\text{B.6a})$$

and for $\lambda < \frac{1}{4}$

$$f(\lambda) = \frac{1}{2} \left(\ln \frac{\eta^+}{\eta^-} \right)^2 - \frac{\pi^2}{2} + i\pi \ln \frac{\eta^+}{\eta^-}, \quad (\text{B.6b})$$

$$\eta^\pm = \frac{1}{2} \pm \sqrt{\frac{1}{4} - \lambda} \quad (\text{B.6c})$$

The subscripts q , l , and W stand for quark, lepton and W -boson, respectively.

$$\lambda_i \equiv \frac{m_i^2}{m_H^2}, \quad \text{for } i = q, l, W, \quad (\text{B.7})$$

and m_i are the rest masses of the corresponding particles. m_H is the rest mass of H^0 .

In the following, we give the derivations of the cross sections for the processes

$$\gamma\gamma \rightarrow s^+s^-, \quad (\text{B.8})$$

$$\gamma\gamma \rightarrow l^+l^-. \quad (\text{B.9})$$

We also give a derivation of the relationship between σ and Γ for the process

$$\gamma\gamma \rightarrow H^0 \quad (\text{B.10})$$

Derivation for $\gamma\gamma \rightarrow s^+s^-$. The lagrangian for the system, including the EM interaction, can be written as

$$\mathcal{L}_{\text{EM}} = - \left(\frac{\partial}{\partial x_\mu} + ieA_\mu \right) \phi^+ \left(\frac{\partial}{\partial x^\mu} - ieA^\mu \right) \phi - m^2 \phi^+ \phi \quad (\text{B.11})$$

in which ϕ denotes a scalar field operator, A_μ denotes the photon field, $\mu = 0, 1, 2, 3$. We use the convention that repeated indices are summed over, so that for example,

$$A_\mu A^\mu = A_0 A^0 + A_1 A^1 + A_2 A^2 + A_3 A^3 \quad (\text{B.12a})$$

$$= A_0 A_0 - A_1 A_1 - A_2 A_2 - A_3 A_3. \quad (\text{B.12b})$$

This lagrangian can be separated into a free part, and an interaction part, so that

$$\begin{aligned} \mathcal{L}_{\text{int}} = ie \left(\phi^+ A^\mu \frac{\partial \phi}{\partial x^\mu} - \frac{\partial \phi^+}{\partial x_\mu} A_\mu \phi \right) \\ + e^2 A^\mu A_\mu \phi^+ \phi. \end{aligned} \quad (\text{B.13})$$

To simplify notations, in this derivation, we are using m instead of m_s to denote the mass of the scalar particle. The S -matrix element that contributes to (B.8) can be written in the form

$$\langle p_-, p_+ | S^{(1)} + S^{(2)} | k_1, \epsilon_1; k_2, \epsilon_2 \rangle \quad (\text{B.14})$$

in which p_\pm denotes the momenta of s^\pm , k_i, ϵ_i are the momenta and polarization vectors of the photons, $i = 1, 2$, and $S^{(2)}$ is defined by

$$S^{(2)} = \frac{i^2}{2} T \int \mathcal{L}_{\text{int}}(x_1) \mathcal{L}_{\text{int}}(x_2) d^4 x_1 d^4 x_2, \quad (\text{B.15})$$

where T denotes the time-ordering operator. Contribution from $S^{(2)}$ can be represented by the diagrams of Figures B.1a and B.1b.

Using (B.13) and (B.15), and standard techniques of field theory, one obtains

$$\begin{aligned} & \langle p_-, p_+ | S^{(2)} | k_1, \epsilon_1; k_2, \epsilon_2 \rangle \\ &= ie^2 (2\pi)^4 (2p_{-0} \cdot 2p_{+0} \cdot 2k_{10} \cdot 2k_{20})^{-\frac{1}{2}} \Omega^{-2} \\ & \times \left[\frac{\epsilon_1^\mu (k_\mu + p_{-\mu}) \epsilon_2^\nu (p_{+\nu} - k_\nu)}{k^2 - m^2 + i\epsilon} + \frac{\epsilon_2^\mu (k'_\mu + p_{-\mu}) \epsilon_1^\nu (p_{+\nu} - k'_\nu)}{k'^2 - m^2 + i\epsilon} \right] \\ & \times \delta^4(p_- + p_+ - k_1 - k_2), \end{aligned} \quad (\text{B.16})$$

where $k \equiv p_- - k_1 = k_2 - p_+$, $k' \equiv p_- - k_2 = k_1 - p_+$, Ω is the normalization volume, and ϵ denotes an infinitesimal quantity.

Likewise $S^{(1)}$ is defined by

$$S^{(1)} = i T \int \mathcal{L}_{\text{int}}(x) d^4k, \quad (\text{B.17})$$

and

$$\begin{aligned} \langle p_-; p_+ | S^{(1)} | k_1, \epsilon_1; k_2, \epsilon_2 \rangle &= i e^2 (2\pi)^4 (2p_{-o} \cdot 2p_{+o} \cdot 2k_{10} \cdot 2k_{20})^{-1/2} \\ &\times \Omega^{-2} 2\epsilon_1 \cdot \epsilon_2 \delta^4(p_- + p_+ - k_1 - k_2). \end{aligned} \quad (\text{B.18})$$

The diagram representing this matrix element is shown in figure B.2.

The total cross section is obtained by squaring (B.14), averaging over photon polarizations ϵ_1 and ϵ_2 , integrating over phase space, and finally dividing by the photon flux. Hence we have

$$\begin{aligned} \sigma &= \int \frac{1}{4} \sum_{\epsilon_1, \epsilon_2} \left| \langle p_-; p_+ | S^{(1)} + S^{(2)} | k_1, \epsilon_1; k_2, \epsilon_2 \rangle \right|^2 \frac{d^3p_- d^3p_+}{(2\pi)^6} \\ &\times \Omega^2 \times \frac{\Omega}{2c} \times \frac{1}{T_o}, \end{aligned} \quad (\text{B.19})$$

in which T_o is the normalization time. Substituting (B.16) and (B.18) into (B.19), we obtain

$$\begin{aligned} \sigma &= e^4 a^2 \int f(\theta) \delta^4(p_- + p_+ - k_1 - k_2) \frac{\Omega T_o}{(2\pi)^4} \frac{d^3p_- d^3p_+}{(2\pi)^6} \frac{\Omega^3}{2c T_o} \\ &= \frac{e^4 a^2 \Omega^4}{(2\pi)^4 \cdot 2c \cdot (2\pi)^6} (p_{-o}^2 - m^2)^{1/2} \frac{p_{-o}}{2} \int_0^\pi f(\theta) \sin \theta d\theta \times 2\pi. \end{aligned} \quad (\text{B.20})$$

where

$$\begin{aligned} f(\theta) &\equiv \frac{1}{4} \sum_{\epsilon_1, \epsilon_2} \left[\frac{\epsilon_1 \cdot (k + p_-) \epsilon_2 \cdot (p_+ - k)}{k^2 - m^2 + i\epsilon} \right. \\ &\quad \left. + \frac{\epsilon_2 \cdot (k' + p_-) \epsilon_1 \cdot (p_+ - k')}{k'^2 - m^2 + i\epsilon} + 2\epsilon_1 \cdot \epsilon_2 \right]^2, \end{aligned} \quad (\text{B.21})$$

$$a \equiv (2\pi)^4 (2p_{-o} \cdot 2p_{+o} \cdot 2k_{10} \cdot 2k_{20})^{-\frac{1}{2}} \Omega^{-2}, \quad (\text{B.22})$$

and θ is the angle between \vec{p}_- and the z-axis, which is chosen to be along the direction of \vec{k}_1 . We shall work in the center of momentum frame of the two photons, and use the fact that for real photons,

$$\epsilon_1 \cdot k_1 = \epsilon_2 \cdot k_2 = 0. \quad (\text{B.23})$$

After some algebraic manipulation, we obtain

$$f(\theta) = \beta^4 \sin^4 \theta \left[\frac{1}{(1 - \beta \cos \theta)^2} + \frac{2}{(1 - \beta \cos \theta)(1 + \beta \cos \theta)} + \frac{1}{(1 + \beta \cos \theta)^2} \right] \\ + 2 - 2\beta^2 \sin^2 \theta \left[\frac{1}{1 - \beta \cos \theta} + \frac{1}{1 + \beta \cos \theta} \right],$$

in which

$$\beta \equiv \frac{|\vec{p}_-|}{p_- o}. \quad (\text{B.24})$$

(B.20) can be simplified by carrying out the integration over θ , so that

$$\int_0^\pi f(\theta) \sin \theta d\theta = 4(2 - \beta^2) + 2(\beta^2 + 1)(\beta^2 - 1) \frac{1}{\beta} \ln \left| \frac{1 + \beta}{1 - \beta} \right|, \quad (\text{B.25})$$

and hence

$$\sigma = \frac{e^4 a^2 \Omega^4}{(2\pi)^{10} \cdot 2c} \frac{p_-^2 o}{2} \beta \times 2\pi \\ \times \left[4(2 - \beta^2) + 2(\beta^2 + 1)(\beta^2 - 1) \frac{1}{\beta} \ln \left| \frac{1 + \beta}{1 - \beta} \right| \right]. \quad (\text{B.26})$$

Using the definition of a in (B.22), we then obtain

$$\sigma = e^4 (2\pi)^8 \Omega^{-4} \frac{1}{16p_-^4} \frac{\Omega^4}{(2\pi)^{10} \times 2c} \times \frac{p_-^2 o}{2} \times 2\pi \times \left[4(2 - \beta^2)\beta \right. \\ \left. + 2(\beta^2 + 1)(\beta^2 - 1) \ln \left| \frac{1 + \beta}{1 - \beta} \right| \right] \quad (\text{B.27a})$$

$$= \frac{e^4}{(2\pi)^2} \frac{1}{16p_-^2} \frac{1}{4c} \times 2\pi \times \left[4(2 - \beta^2)\beta + 2(\beta^2 + 1)(\beta^2 - 1) \right. \\ \left. \times \ln \left| \frac{1 + \beta}{1 - \beta} \right| \right]. \quad (\text{B.27b})$$

In the “natural units” in which one sets $\hbar = c = 1$, this result can be written in the form

$$\sigma = \frac{e^4}{(4\pi)^2} \frac{1}{4p_-^2 o} \times 2\pi \left[(2 - \beta^2)\beta + (\beta^2 + 1)(\beta^2 - 1) \times \frac{1}{2} \ln \left| \frac{1 + \beta}{1 - \beta} \right| \right]. \quad (\text{B.28})$$

In terms of the variables $y \equiv \frac{4m^2}{W^2}$, $W \equiv p_{-o} + p_{+o} = 2p_{-o}$, we can write

$$\sigma = \alpha^2 \times \frac{1}{W^2} \times 2\pi \left[(1+y)\sqrt{1-y} - (2-y)y \ln \left| \frac{1}{\sqrt{y}} + \sqrt{\frac{1}{y} - 1} \right| \right] \quad (\text{B.29})$$

in which $\alpha \equiv \frac{e^2}{4\pi}$ is the fine structure constant. This result is the same as the one obtained by Papageorgiu (ref. 2, eq. (15), p. 159).

Derivation for $\gamma\gamma \rightarrow l^+l^-$. For this case the interaction lagrangian can be written in the form

$$\mathcal{L}_{\text{int}} = -e \bar{\psi}(x) \mathcal{A}(x)\psi(x), \quad (\text{B.30})$$

in which $\psi(x)$ denotes the lepton field operator. $\mathcal{A}(x) = A_\mu(x)\gamma^\mu$ and γ^μ , $\mu = 0, 1, 2, 3$, are the Dirac γ -matrices. (See ref. 9, Appendix 2, p. 335–361.) $\bar{\psi}(x) = \psi^\dagger(x)\gamma_0$, where $\psi^\dagger(x)$ is the hermitian conjugate of $\psi(x)$. The second order term in the S -matrix is defined by (B.15), with $\mathcal{L}_{\text{int}}(x)$ defined by (B.30). The initial and final states can be denoted as

$$|i\rangle = |k_1, \epsilon_1; k_2, \epsilon_2\rangle, \quad (\text{B.31a})$$

$$|f\rangle = |p_-, s_-; p_+, s_+\rangle, \quad (\text{B.31b})$$

in which we have already defined $k_j, \epsilon_j, j = 1, 2$ as the photon momenta and polarization. p_\pm, s_\pm are the momenta and spins of l^+ and l^- respectively. Following the notations of reference 9, appendix 2, we can write the S -matrix element $\langle f|S^{(2)}|i\rangle$ as

$$\begin{aligned} \langle f|S^{(2)}|i\rangle = & -e^2 a \left[\bar{u}(p_-, s_-) \not{\epsilon}_1 \frac{i(\not{k} + m)}{k^2 - m^2 + i\epsilon} \not{\epsilon}_2 v(p_+, s_+) \right. \\ & \left. + \bar{u}(p_-, s_-) \not{\epsilon}_2 \frac{i(\not{k}' + m)}{k'^2 - m^2 + i\epsilon} \not{\epsilon}_1 v(p_+, s_+) \right] \delta^4(p_- + p_+ - k_1 - k_2), \end{aligned}$$

where

$$k \equiv p_- - k_1 = k_2 - p_+, \quad k' \equiv p_- - k_2 = k_1 - p_+, \quad (\text{B.32})$$

$$a \equiv (2\pi)^4 (2p_{-o} \cdot 2p_{+o} \cdot 2k_{10} \cdot 2k_{20})^{-1/2} \Omega^{-2},$$

$u(p_-, s_-)$ and $v(p_+, s_+)$ are the spinor wave-functions associated with l^- and l^+ . For simplicity of notations, in this derivation we use m instead of m_l to denote the mass of the lepton. This S -matrix element can also be represented diagrammatically by Figures (B.1a) and (B.1b). The total cross section is given by a formula similar to (B.19):

$$\sigma = \int \frac{1}{4} \sum_{\substack{\epsilon_1, \epsilon_2, \\ s_-, s_+}} \left| \langle f | S^2 | i \rangle \right|^2 \frac{d^3 p_- d^3 p_+}{(2\pi)^6} \Omega^2 \frac{\Omega}{2c T_o}. \quad (\text{B.33})$$

Performing the sum over the photon and lepton spins, we can write

$$\begin{aligned} \sum_{\substack{\epsilon_1, \epsilon_2, \\ s_-, s_+}} \left| \langle f | S^{(2)} | i \rangle \right|^2 &= \sum_{\epsilon_1, \epsilon_2} e^4 a^2 \delta^4(p_- + p_+ - k_1 - k_2) \frac{\Omega T_o}{(2\pi)^4} \{(k^2 - m^2 + i\epsilon)^{-2} \\ &\times \text{Tr}[(\not{p}_- + m) \not{\epsilon}_1 (\not{k} + m) \not{\epsilon}_2 (\not{p}_+ - m) \not{\epsilon}_2 (-i)(\not{k} + m) \not{\epsilon}_1] \\ &+ (k^2 - m^2 + i\epsilon)^{-1} (k'^2 - m^2 + i\epsilon)^{-1} \text{Tr}[(\not{p}_- + m) \not{\epsilon}_1 (\not{k} + m) \not{\epsilon}_2 (\not{p}_+ - m) \not{\epsilon}_1 (\not{k}' + m) \not{\epsilon}_2] \\ &+ (k^2 - m^2 + i\epsilon)^{-1} (k'^2 - m^2 + i\epsilon)^{-1} \text{Tr}[(\not{p}_- + m) \not{\epsilon}_2 (\not{k}' + m) \not{\epsilon}_1 (\not{p}_+ - m) \not{\epsilon}_2 (\not{k} + m) \not{\epsilon}_1] \\ &+ (k'^2 - m^2 + i\epsilon)^{-2} \text{Tr}[(\not{p}_- + m) \not{\epsilon}_2 (\not{k}' + m) \not{\epsilon}_1 (\not{p}_+ - m) \not{\epsilon}_1 (\not{k}' + m) \not{\epsilon}_2]\} \end{aligned} \quad (\text{B.34})$$

in which Tr denotes the trace operator. From (B.34), it can be seen that the sum in (B.34) can be naturally divided into four terms:

$$T_1 \equiv \text{Tr}[(\not{p}_- + m) \not{\epsilon}_1 (\not{k} + m) \not{\epsilon}_2 (\not{p}_+ - m) \not{\epsilon}_2 (\not{k} + m) \not{\epsilon}_1], \quad (\text{B.35a})$$

$$T_2 \equiv \text{Tr}[(\not{p}_- + m) \not{\epsilon}_1 (\not{k} + m) \not{\epsilon}_2 (\not{p}_+ - m) \not{\epsilon}_1 (\not{k}' + m) \not{\epsilon}_2], \quad (\text{B.35b})$$

$$T_3 \equiv \text{Tr}[(\not{p}_- + m) \not{\epsilon}_2 (\not{k}' + m) \not{\epsilon}_1 (\not{p}_+ - m) \not{\epsilon}_2 (\not{k} + m) \not{\epsilon}_1], \quad (\text{B.35c})$$

$$T_4 \equiv \text{Tr}[(\not{p}_- + m) \not{\epsilon}_2 (\not{k}' + m) \not{\epsilon}_1 (\not{p}_+ - m) \not{\epsilon}_1 (\not{k}' + m) \not{\epsilon}_2]. \quad (\text{B.35d})$$

Hence we can write

$$\begin{aligned}
& \sum_{\substack{\epsilon_1, \epsilon_2, \\ s_-, s_+}} \left| \langle f | S^{(2)} | i \rangle \right|^2 = e^4 a^2 \delta^4(p_- + p_+ - k_1 - k_2) \frac{\Omega T_o}{(2\pi)^4} \\
& \times \sum_{\epsilon_1, \epsilon_2} \{ (k^2 - m^2 + i\epsilon)^{-2} T_1 + (k^2 - m^2 + i\epsilon)^{-1} (k'^2 - m^2 + i\epsilon)^{-1} (T_2 + T_3) \\
& + (k'^2 - m^2 + i\epsilon)^{-2} T_4 \}. \tag{B.36}
\end{aligned}$$

After some straight forward though tedious mathematics, one arrives at the following:

$$\frac{1}{4} \sum_{\epsilon_1, \epsilon_2} T_1 = 8k_{10}^4 (1 - \beta \cos \theta) \left(1 + \frac{m^2}{k_{10}^2} + \frac{2m^2}{k_{10}^2} \beta \cos \theta + \beta^3 \cos^3 \theta \right) - 8m^4, \tag{B.37}$$

$$\frac{1}{4} \sum_{\epsilon_1, \epsilon_2} T_2 = \frac{1}{4} \sum_{\epsilon_1, \epsilon_2} T_3 = 8k_{10}^4 \beta^2 (1 - \cos^2 \theta) \left[1 - \beta^2 (1 - \cos^2 \theta) \right], \tag{B.38}$$

$$\frac{1}{4} \sum_{\epsilon_1, \epsilon_2} T_4 = 8k_{10}^4 (1 + \beta \cos \theta) \left(1 + \frac{m^2}{k_{10}^2} - \frac{2m^2}{k_{10}^2} \beta \cos \theta - \beta^3 \cos^3 \theta \right) - 8m^4, \tag{B.39}$$

where $\beta \equiv \frac{|\vec{p}_-|}{p_-}$. From (B.33) and (B.36) we obtain

$$\begin{aligned}
\sigma &= e^4 (2\pi)^8 (2k_{10})^{-4} \Omega^{-4} \frac{\Omega T_o}{(2\pi)^4} \frac{\Omega^3}{(2\pi)^6} \frac{1}{2cT_o} \\
& \times \int \left\{ \frac{1}{4} \sum_{\epsilon_1, \epsilon_2} [(k^2 - m^2 + i\epsilon)^{-2} T_1 + (k^2 - m^2 + i\epsilon)^{-1} (k'^2 - m^2 + i\epsilon)^{-1} (T_2 + T_3) \right. \\
& \left. + (k'^2 - m^2 + i\epsilon)^{-2} T_4 \right\} d^3 p_- d^3 p_+ \delta^4(p_- + p_+ - k_1 - k_2) \\
&= \frac{e^4}{(2\pi)^2} \frac{1}{16k_{10}^4} \frac{1}{2c} \beta k_{10}^2 \times \int \left\{ \frac{1}{4} \sum_{\epsilon_1, \epsilon_2} [(k^2 - m^2 + i\epsilon)^{-2} T_1 \right. \\
& \left. + (k^2 - m^2 + i\epsilon)^{-1} (k'^2 - m^2 + i\epsilon)^{-1} (T_2 + T_3) + (k'^2 - m^2 + i\epsilon)^{-2} T_4 \right\} \\
& \times \frac{1}{2} \sin \theta d\theta \times 2\pi. \tag{B.40}
\end{aligned}$$

Now we use

$$k^2 - m^2 = -2k_{10}^2 (1 - \beta \cos \theta), \tag{B.41}$$

$$k'^2 - m^2 = -2k_{10}^2(1 + \beta \cos \theta), \quad (\text{B.42})$$

together with (B.37), (B.38), and (B.39) to arrive at

$$\begin{aligned} \int_0^\pi \frac{1}{4} \sum_{\epsilon_1, \epsilon_2} (k^2 - m^2 + i\epsilon)^{-2} T_1 \sin \theta \, d\theta &= \int_0^\pi \frac{1}{4} \sum_{\epsilon_1, \epsilon_2} (k'^2 - m^2 + i\epsilon)^{-2} T_4 \sin \theta \, d\theta \\ &= -\frac{4}{3} \beta^2 - 4 - 8 \frac{m^2}{k_{10}^2} + 2 \left(2 + \frac{3m^2}{k_{10}^2} \right) \frac{1}{\beta} \ln \left| \frac{1+\beta}{1-\beta} \right| - \frac{4m^4}{k_{10}^4} \frac{1}{1-\beta^2}, \end{aligned} \quad (\text{B.43})$$

$$\begin{aligned} &\int_0^\pi \frac{1}{4} \sum_{\epsilon_1, \epsilon_2} (k^2 - m^2 + i\epsilon)^{-1} (k'^2 - m^2 + i\epsilon)^{-1} T_2 \sin \theta \, d\theta \\ &= \int_0^\pi \frac{1}{4} \sum_{\epsilon_1, \epsilon_2} (k^2 - m^2 + i\epsilon)^{-1} (k'^2 - m^2 + i\epsilon)^{-1} T_3 \sin \theta \, d\theta \\ &= 8(1 - \beta^2) + \frac{4}{3} \beta^2 - \frac{2}{\beta} (2 - \beta^2) (1 - \beta^2) \ln \left| \frac{1+\beta}{1-\beta} \right|. \end{aligned} \quad (\text{B.44})$$

So from (B.43) and (B.44) we have

$$\begin{aligned} &\int_0^\pi \frac{1}{4} \sum_{\epsilon_1, \epsilon_2} [(k^2 - m^2 + i\epsilon)^{-2} T_1 + (k^2 - m^2 + i\epsilon)^{-1} (k'^2 - m^2 + i\epsilon)^{-1} (T_2 + T_3) \\ &\quad + (k'^2 - m^2 + i\epsilon)^{-2} T_4] \sin \theta \, d\theta \\ &= -8(2 - \beta^2) + \frac{4}{\beta} [2 + 3(1 - \beta^2) - (2 - \beta^2)(1 - \beta^2)] \ln \left| \frac{1+\beta}{1-\beta} \right| \\ &= -8(1 + y) + \frac{16}{\beta} \left(1 + y - \frac{y^2}{2} \right) \ln \left| \frac{1}{\sqrt{y}} + \sqrt{\frac{1}{y} - 1} \right|, \end{aligned} \quad (\text{B.45})$$

where $y \equiv \frac{4m^2}{W^2} = 1 - \beta^2$. Putting this into (B.40), we have

$$\begin{aligned} \sigma &= \frac{e^4}{(2\pi)^2} \frac{1}{16k_{10}^4} \frac{1}{2c} \beta k_{10}^2 \times 8 \left[-(1 + y) + \frac{2}{\beta} \left(1 + y - \frac{y^2}{2} \right) \right. \\ &\quad \left. \times \ln \left| \frac{1}{\sqrt{y}} + \sqrt{\frac{1}{y} - 1} \right| \right] \times \frac{2\pi}{2} \\ &= \frac{e^4}{(4\pi)^2} \frac{1}{W^2} \times 4\pi \left[-(1 + y) \sqrt{1 - y} + 2 \left(1 + y - \frac{y^2}{2} \right) \ln \left| \frac{1}{\sqrt{y}} + \sqrt{\frac{1}{y} - 1} \right| \right] \\ &= \frac{\alpha^2}{W^2} \times 4\pi \left[-(1 + y) \sqrt{1 - y} + 2 \left(1 + y - \frac{y^2}{2} \right) \ln \left| \frac{1}{\sqrt{y}} + \sqrt{\frac{1}{y} - 1} \right| \right], \end{aligned} \quad (\text{B.46})$$

in “natural” units. This result is the same as the one obtained by Papageorgiu (ref. 2, eq. (14), p. 159).

Derivation for $\gamma\gamma \rightarrow s^o$

s^o is a neutral scalar. Using p_s to denote the momentum of s^o , the cross section for this process can be written as

$$\sigma = \int \frac{1}{4} = \sum_{\epsilon_1, \epsilon_2} \left| \langle p_s | S | k_1, \epsilon_1; k_2, \epsilon_2 \rangle \right|^2 \frac{d^3 p_s}{(2\pi)^3} \Omega \times \frac{\Omega}{2c} \times \frac{1}{T_o}, \quad (\text{B.47})$$

in which S denotes the S -matrix. For the reverse decay process $s^o \rightarrow \gamma\gamma$, the width Γ can be written in the form

$$\Gamma = \frac{1}{T_o} \int \sum_{\epsilon_1, \epsilon_2} \left| \langle k_1, \epsilon_1; k_2, \epsilon_2 | S | p_s \rangle \right|^2 \frac{d^3 k_1 d^3 k_2}{(2\pi)^6} \Omega^2 \quad (\text{B.48})$$

From conservation of momentum, we can write

$$\langle p_s | S | k_1, \epsilon; k_2, \epsilon_2 \rangle = \langle p_s | T | k_1, \epsilon_1; k_2, \epsilon_2 \rangle \delta^4(p_s - k_1 - k_2) \quad (\text{B.49})$$

From (B.47) and (B.49) we now have

$$\begin{aligned} \sigma &= \frac{1}{4} \sum_{\epsilon_1, \epsilon_2} \left| \langle p_s | T | k_1, \epsilon_1; k_2, \epsilon_2 \rangle \right|^2 \delta(p_{s0} - k_{10} - k_{20}) \\ &\quad \times \frac{1}{(2\pi)^3} \frac{\Omega^2}{2cT_o} \frac{\Omega T_o}{(2\pi)^4} \end{aligned} \quad (\text{B.50a})$$

$$= \frac{1}{8c(2\pi)^7} \sum_{\epsilon_1, \epsilon_2} \left| \langle p_s | T | k_1, \epsilon_1; k_2, \epsilon_2 \rangle \right|^2 \delta(p_{s0} - 2k_1) \quad (\text{B.50b})$$

In (B.50), we assume that we are working in the rest frame of s^o . Likewise (B.48) can also be rewritten in the form

$$\begin{aligned} \Gamma &= \frac{1}{T_o} \sum_{\epsilon_1, \epsilon_2} \left| \langle k_1, \epsilon_1; k_2, \epsilon_2 | T | p_s \rangle \right|^2 \frac{k_{10}^2}{2} \times 4\pi \times \frac{\Omega^2}{(2\pi)^6} \frac{\Omega T_o}{(2\pi)^4} \\ &= \frac{\Omega^3}{(2\pi)^9} k_{10}^2 \sum_{\epsilon_1, \epsilon_2} \left| \langle k_1, \epsilon_1; k_2, \epsilon_2 | T | p_s \rangle \right|^2 \end{aligned} \quad (\text{B.51})$$

From time-reversal invariance, we know that

$$\sum_{\epsilon_1, \epsilon_2} \left| \langle k_1, \epsilon_1; k_2, \epsilon_2 | T | p_s \rangle \right|^2 = \sum_{\epsilon_1, \epsilon_2} \left| \langle p_s | T | k_1, \epsilon_1; k_2, \epsilon_2 \rangle \right|^2. \quad (\text{B.52})$$

Therefore from (B.50) and (B.51) we now have

$$\sigma = \frac{1}{8c} (2\pi)^2 \Gamma \times \frac{1}{k_{10}^2} \delta(p_{s0} - 2k_{10}). \quad (\text{B.53})$$

In the rest frame of s^0 ,

$$\sigma = (2\pi)^2 \Gamma \frac{1}{k_{10}} \delta(m_s^2 - 4k_{10}^2) = \frac{8\pi^2}{m_s} \Gamma \delta(m_s^2 - s), \quad (\text{B.54})$$

in which s is the square of the total momentum $(k_1 + k_2)^2$. For $\gamma\gamma \rightarrow H^0$ in which H^0 is a neutral Higgs particle, Γ can be written in the form given by (B.4)-(B.7).

Appendix C. Fermion Contribution to $\Gamma(H^o \rightarrow \gamma\gamma)$.

In this appendix, we derive the Fermion contribution to the decay width of the decay of a Higgs particle $H^o \rightarrow \gamma\gamma$. For this case the interaction lagrangian can be written as (ref. 14, eqs. (22.58), (22.78), pp. 676, 682)

$$\mathcal{L}_{\text{int}}(x) = \mathcal{L}_{\text{int}}^{(e)}(x) + \mathcal{L}_{\text{int}}^{(h)}(x), \quad (\text{C.1a})$$

where

$$\mathcal{L}_{\text{int}}^{(e)}(x) = q_f \bar{\psi}_f A(x) \psi_f(x), \quad \mathcal{L}_{\text{int}}^{(h)}(x) = h_f \bar{\psi}_f(x) \eta(x) \psi_f(x). \quad (\text{C.1b})$$

$\psi_f(x)$ is the fermion field operator, $A_\mu(x)$ the photon field operator, and $\eta(x)$ the scalar Higgs field operator. q_f denotes the charge of the fermion, and h_f the coupling between the Higgs scalar and the fermion. The process $H^o \rightarrow \gamma\gamma$ is third order in the interaction, so that the relevant term in the S -matrix is

$$S^{(3)} = \frac{i^3}{3!} T \left[\int \mathcal{L}_{\text{int}}(x_1) \mathcal{L}_{\text{int}}(x_2) \mathcal{L}_{\text{int}}(x_3) d^4x_1 d^4x_2 d^4x_3 \right] \quad (\text{C.2})$$

The initial and final states can be denoted as

$$|i\rangle = |p_h\rangle, \quad \text{and} \quad |f\rangle = |k_1, \epsilon_1; k_2, \epsilon_2\rangle, \quad (\text{C.3})$$

in which p_h denotes the momentum of the Higgs scalar, $k_j, \epsilon_j, j = 1, 2$, are the momenta and polarizations of the photons.

We use m_f and m_H to denote the masses of the fermion and Higgs scalar. The width for the process is given by

$$\Gamma = \frac{1}{T_o} \frac{1}{4} \int \sum_{\epsilon_1, \epsilon_2} \left| \langle k_1, \epsilon_1; k_2, \epsilon_2 | S^{(3)} | p_h \rangle \right|^2 \frac{d^3k_1 d^3k_2}{(2\pi)^6} \Omega^2. \quad (\text{C.4})$$

The S -matrix element can be represented by the diagrams:

Employing standard techniques of field theory, we find

$$\begin{aligned}
\langle k_1, \epsilon_1; k_2, \epsilon_2 | S^{(3)} | p_h \rangle &= -q_f^2 h_f (2p_{h_o} \cdot 2k_{10} \cdot 2k_{20})^{-1/2} \Omega^{-3/2} \\
&\times \int d^4 p_1 \left\{ \left[(p_1 - k_1)^2 - m_f^2 + i\epsilon \right]^{-1} \text{Tr} \left[(p_1 + m_f) \not{\epsilon}_1 (\not{p}_1 - \not{k}_1 + m_f) \not{\epsilon}_2 (\not{p}_1 - \not{k}_1 - \not{k}_2 + m_f) \right] \right. \\
&+ \left. \left[(p_1 - k_2)^2 - m_f^2 + i\epsilon \right]^{-1} \text{Tr} \left[(\not{p}_1 + m_f) \not{\epsilon}_2 (\not{p}_1 - \not{k}_2 + m_f) \not{\epsilon}_1 (\not{p}_1 - \not{k}_1 - \not{k}_2 + m_f) \right] \right\} \\
&\times (p_1^2 - m_f^2 + i\epsilon)^{-1} \left[(p_1 - k_1 - k_2)^2 - m_f^2 + i\epsilon \right]^{-1} \delta^4(k_1 + k_2 - p_h). \tag{C.5}
\end{aligned}$$

We can separate the two terms on the right hand side of (C.5) and let $S^{(3)} = S_1^{(3)} + S_2^{(3)}$,

so that

$$\begin{aligned}
\langle k_1, \epsilon_1; k_2, \epsilon_2 | S_1^{(3)} | p_h \rangle &= -q_f^2 h_f (2p_{h_o} \cdot 2k_{10} \cdot 2k_{20})^{-1/2} \Omega^{-3/2} \delta^4(k_1 + k_2 - p_h) \\
&\times \int d^4 p_1 \left[(p_1 - k_1)^2 - m_f^2 + i\epsilon \right]^{-1} (p_1^2 - m_f^2 + i\epsilon)^{-1} \\
&\times \left[(p_1 - k_1 - k_2)^2 - m_f^2 + i\epsilon \right]^{-1} T_1^{(3)}, \tag{C.6a}
\end{aligned}$$

where

$$T_1^{(3)} \equiv \text{Tr} \left[(\not{p}_1 + m_f) \not{\epsilon}_1 (\not{p}_1 - \not{k}_1 + m_f) \not{\epsilon}_2 (\not{p}_1 - \not{k}_1 - \not{k}_2 + m_f) \right], \tag{C.6b}$$

and

$$\begin{aligned}
\langle k_1, \epsilon_1; k_2, \epsilon_2 \mid S_2^{(3)} \mid p_h \rangle &= -q_f^2 h_f (2p_{h_0} \cdot 2k_{10} \cdot 2k_{20})^{-1/2} \Omega^{-3/2} \delta^4(k_1 + k_2 - p_h) \\
&\times \int d^4 p_1 \left[(p_1 - k_2)^2 - m_f^2 + i\epsilon \right]^{-1} \left[p_1^2 - m_f^2 + i\epsilon \right]^{-1} \\
&\times \left[(p_1 - k_1 - k_2)^2 - m_f^2 + i\epsilon \right]^{-1} T_2^{(3)}, \tag{C.7}
\end{aligned}$$

where

$$T_2^{(3)} \equiv \text{Tr} \left[(\not{p}_1 + m_f) \not{\epsilon}_2 (\not{p}_1 - \not{k}_2 + m_f) \not{\epsilon}_1 (\not{p}_1 - \not{k}_1 - \not{k}_2 + m_f) \right]. \tag{C.8}$$

The evaluation of the matrix elements (C.6) and (C.7) are quite similar. So we need only consider (C.6) in detail for illustration. By evaluating the trace in (C.6b), and using the fact that in the center of momentum frame of the two photons,

$$\epsilon_1 \cdot k_1 = \epsilon_1 \cdot k_2 = \epsilon_2 \cdot k_1 = \epsilon_2 \cdot k_2 = 0, \tag{C.9}$$

and also

$$k_1^2 = k_2^2 = 0, \tag{C.10}$$

for real photons, we find

$$\begin{aligned}
T_1^{(3)} &= 4m_f (4p_1 \cdot \epsilon_1 p_1 \cdot \epsilon_2 - \epsilon_1 \cdot \epsilon_2 p_1^2) + 8m_f \epsilon_1 \cdot \epsilon_2 p_1 \cdot k_1 \\
&+ 4m_f (-k_1 \cdot k_2 + m_f^2) \epsilon_1 \cdot \epsilon_2. \tag{C.11}
\end{aligned}$$

Now we use a standard technique of Feynman parameterization (ref. 15, Section 3.2, pp. 160–197).

$$\begin{aligned}
&(p_1^2 - m^2 + i\epsilon)^{-1} \left[(p_1 - k_1)^2 - m^2 + i\epsilon \right]^{-1} \left[(p_1 - k_1 - k_2)^2 - m^2 + i\epsilon \right]^{-1} \\
&= 2 \int_0^1 dx \int_0^{1-x} dy \left[(p_1 - Q)^2 + \rho_1^2 \right]^{-3} \tag{C.12a}
\end{aligned}$$

where

$$Q^\mu \equiv x k_1^\mu + y (k_1^\mu + k_2^\mu), \tag{C.12b}$$

$$\begin{aligned}
\rho_1^2 &\equiv -Q^2 - m_f^2 + k_1^2 x + (k_1 + k_2)^2 y + i\epsilon \\
&\equiv -Q^2 - m_f^2 + 2k_1 \cdot k_2 y + i\epsilon.
\end{aligned} \tag{C.12c}$$

Now (C.6) can be rewritten in the form

$$\begin{aligned}
\langle k_1, \epsilon_1; k_2, \epsilon_2 | S_1^{(3)} | p_h \rangle &= -q_f^2 h_f (2p_{h_o} \cdot 2k_{10} \cdot k_{20})^{-1/2} \Omega^{-3/2} \delta^4(k_1 + k_2 - p_h) \\
&\times 2 \int_0^1 dx \int_0^{1-x} dy \int d^4 p_1 [(p_1 - Q)^2 + \rho_1^2]^{-3} T_1^{(3)}.
\end{aligned} \tag{C.13}$$

From (C.11) and (C.13), it is apparent that in order to evaluate (C.13) we need to compute the following integrals:

$$I_2^{\mu\nu} \equiv \int dx dy d^4 p_1 p_1^\mu p_1^\nu [(p_1 - Q)^2 + \rho_1^2]^{-3}, \tag{C.14}$$

$$I_1^\mu \equiv \int dx dy d^4 p_1 p_1^\mu [(p_1 - Q)^2 + \rho_1^2]^{-3}, \tag{C.15}$$

$$I_o \equiv \int dx dy d^4 p_1 [(p_1 - Q)^2 + \rho_1^2]^{-3}. \tag{C.16}$$

These integrals can be computed using the method of dimensional regularization in which one first computes the following integrals:

$$I_2^{\mu\nu}(n) \equiv \int dx dy d^n p_1 p_1^\mu p_1^\nu [(p_1 - Q)^2 + \rho_1^2]^{-3}, \tag{C.17}$$

$$I_1^\mu(n) \equiv \int dx dy d^n p_1 p_1^\mu [(p_1 - Q)^2 + \rho_1^2]^{-3}, \tag{C.18}$$

$$I_o(n) \equiv \int dx dy d^n p_1 [(p_1 - Q)^2 + \rho_1^2]^{-3}, \tag{C.19}$$

in which n is a real number, which in the final result is allowed to approach 4. Details of this process is given in Appendix D.

From the results in Appendix D, we find

$$\int d^4 p_1 \frac{4p_1^\mu p_1^\nu - p_1^2 g^{\mu\nu}}{[(p_1 - Q)^2 + \rho_1^2]^3} = -i \frac{\pi^2}{2} \frac{1}{\rho_1^2} [g^{\mu\nu}(\rho_1^2 - Q^2) + 4Q^\mu Q^\nu], \tag{C.20}$$

$$\int d^4 p_1 \frac{p_1^\mu}{[(p_1 - Q)^2 + \rho_1^2]^3} = -i \frac{\pi^2}{2} \frac{Q^\mu}{\rho_1^2}, \tag{C.21}$$

and

$$\int d^4 p_1 \frac{1}{[(p_1 - Q)^2 + \rho_1^2]^3} = -i \frac{\pi^2}{2} \frac{1}{\rho_1^2}. \quad (\text{C.22})$$

Define

$$J_1 \equiv \int d^4 p_1 \left[(p_1 - k_1)^2 - m_f^2 + i\epsilon \right]^{-1} \left(p_1^2 - m_f^2 + i\epsilon \right)^{-1} \\ \times \left[(p_1 - k_1 - k_2)^2 - m_f^2 + i\epsilon \right]^{-1} \times T_1^{(3)}. \quad (\text{C.23})$$

By using (C.9)–(C.12), (C.20)–(C.23), we find

$$J_1 = -i\pi^2 \int_0^1 dx \int_0^{1-y} dy \frac{1}{\rho_1^2} \left[4m_f (\rho_1^2 - Q^2) \right. \\ \left. + 8m_f Q \cdot k_1 + 4m_f (-k_1 \cdot k_2 + m_f^2) \right] \epsilon_1 \cdot \epsilon_2. \quad (\text{C.24})$$

Using the definitions of ρ_1 and Q in (C.11) and (C.12), we can simplify (C.24) to

$$J_1 = -i\pi^2 2m_f \epsilon_1 \cdot \epsilon_2 \int_0^1 dx \int_0^{1-x} dy \frac{4y(1-x-y) - 1}{y(1-x-y) - \lambda + i\epsilon}, \quad (\text{C.25})$$

where $\lambda \equiv \frac{m_f^2}{2k_1 \cdot k_2} = \frac{m_f^2}{m_H^2}$.

The integral in (C.25) can be done after some changes of integration variables and applying some techniques in complex analysis. The result is

$$J_1 = -i\pi^2 2m_f \epsilon_1 \cdot \epsilon_2 J_0, \quad (\text{C.26})$$

where for $\lambda = \frac{m_f^2}{m_H^2} > \frac{1}{4}$,

$$J_0 = 2 - 2(4\lambda - 1) \left[\arcsin \left(\frac{1}{\sqrt{4\lambda}} \right) \right]^2, \quad (\text{C.27a})$$

and for $\lambda \leq \frac{1}{4}$,

$$J_0 = 2 + (4\lambda - 1) \left\{ -\frac{\pi^2}{2} + \frac{1}{2} \left[\ln \left| \frac{\frac{1}{2} + \sqrt{\frac{1}{4} - \lambda}}{\frac{1}{2} - \sqrt{\frac{1}{4} - \lambda}} \right| \right]^2 \right. \\ \left. - i\pi \ln \left| \frac{\frac{1}{2} + \sqrt{\frac{1}{4} - \lambda}}{\frac{1}{2} - \sqrt{\frac{1}{4} - \lambda}} \right| \right\}. \quad (\text{C.27b})$$

From (C.5), (C.6), (C.23) and (C.26) we have therefore

$$\begin{aligned}
\langle k_1, \epsilon_1; k_2, \epsilon_2 | S_1^{(3)} | p_h \rangle &= -q_f^2 h_f (2p_{ho} \cdot 2k_{10} \cdot 2k_{20})^{-1/2} \Omega^{-3/2} J_1 \delta^4(k_1 + k_2 - p_h) \\
&= -q_f^2 h_f (2p_{ho} \cdot 2k_{10} \cdot 2k_{20})^{-1/2} \Omega^{-3/2} \delta^4(k_1 + k_2 - p_h) \\
&\quad \times \left(-i\pi^2 \times 2m_f \times \epsilon_1 \cdot \epsilon_2 J_0 \right). \tag{C.28}
\end{aligned}$$

It is straight forward to check that

$$\langle k_1, \epsilon_1; k_2, \epsilon_2 | S_2^{(3)} | p_h \rangle = \langle k_1, \epsilon_1; k_2, \epsilon_2 | S_1^{(3)} | p_h \rangle. \tag{C.29}$$

Therefore using (C.3)–(C.8) and (C.28),

$$\begin{aligned}
\Gamma &= \frac{1}{T_0} \frac{1}{4} \int \sum_{\epsilon_1, \epsilon_2} 4q_f^4 h_f^2 (2p_{ho} \cdot 2k_{10} \cdot 2k_{20})^{-1} \Omega^{-3} \delta^4(k_1 + k_2 - p_h) \\
&\quad \times \pi^4 \times 4m_f^2 \times (\epsilon_1 \cdot \epsilon_2)^2 |J_0|^2 \times \frac{\Omega T_0}{(2\pi)^4} \frac{d^3 k_1 d^3 k_2 \Omega^2}{(2\pi)^6}. \tag{C.30}
\end{aligned}$$

Now

$$\sum_{\epsilon_1, \epsilon_2} (\epsilon_1 \cdot \epsilon_2)^2 = 2, \quad 2k_{10} = 2k_{20} = p_{ho} = m_H, \tag{C.31}$$

Therefore

$$\begin{aligned}
\Gamma &= \frac{q_f^4 h_f^2}{(2\pi)^{10}} 2 \frac{\pi^4 m_f^2}{m_H^3} 2 |J_0|^2 \int d^3 k_1 \delta(k_{10} + k_{20} - p_{ho}) \\
&= \frac{1}{16 \times (2\pi)^5} q_f^4 h_f^2 m_H \lambda |J_0|^2, \tag{C.32}
\end{aligned}$$

h_f is related to the Fermi coupling constant G_F by $h_f^2 = m_f^2 \times 2\sqrt{2}G_F$ (ref. 14, Section 22.2, eqs. (22.58), (22.70), and (22.83), pp. 676, 679, 684)

$$\begin{aligned}
\Gamma &= \frac{1}{16(2\pi)^5} q_f^4 2\sqrt{2}G_F m_H^3 \lambda^2 |J_0|^2 \\
&= \left| \frac{q_f}{e} \right|^4 \frac{\alpha^2 G_F}{8\sqrt{2}\pi^3} m_H^3 \lambda^2 |J_0|^2. \tag{C.33}
\end{aligned}$$

We note that $\frac{q_f}{e}$ is the charge of the fermion in units of the electron charge. Our result agrees with that in the literature. (See ref. 13, eqs. (10) and (11), p. 95.) We note that the sign of the imaginary part of J_0 in (C.27b) is opposite to that of reference 12, equation (11).

However, since only $|J_o|^2$ enters into quantities of physical interest, such as Γ and σ , therefore this difference in sign of the imaginary part of J_o is not significant.

Appendix D. Evaluation of certain integrals.

In this appendix, we outline the procedures involved in evaluating the integrals in (C.14)–(C.19).

The following integrals can be evaluated by standard methods of calculus.

$$\int_0^\infty \frac{u^m du}{(u^2 + M^2)^\ell} = C_{m,\ell} \times M^{-2\ell+m+1}, \quad (\text{D.1})$$

provided m is even, $m \geq 0$, ℓ is an integer ≥ 0 , $\ell \geq \frac{m}{2} + 1$, and the coefficients $C_{m,\ell}$ are defined by

$$C_{m,\ell} = \frac{(\ell - \frac{m}{2} - 1)!}{(\ell - 1)!} \left(\frac{m-1}{2} \cdot \frac{m-3}{2} \cdots \frac{3}{2} \cdot \frac{1}{2} \right) \times \int_0^{\frac{\pi}{2}} (\cos \theta)^{2\ell-m-2} d\theta \quad (\text{D.2})$$

If ℓ is a half-integer, (D.1) still applies with

$$C_{m,\ell} = \left[(\ell - 1)(\ell - 2) \cdots \left(\ell - \frac{m}{2} \right) \right]^{-1} \left(\frac{m-1}{2} \cdot \frac{m-3}{2} \cdots \frac{1}{2} \right) \times \int_0^{\frac{\pi}{2}} (\cos \theta)^{2\ell-m-2} d\theta. \quad (\text{D.3})$$

Using methods of complex analysis, we can show that the same formula (D.1) applies if M is replaced by iM in (D.1).

$$\int d^n p (p^2 + M^2)^{-\alpha} = \int_{-\infty}^{\infty} dp_o \int_0^\infty |\vec{p}|^{n-2} d|\vec{p}| (p_o^2 - |\vec{p}|^2 + M^2)^{-\alpha} \Omega_{n-2}^{(0)}, \quad (\text{D.4})$$

where $\Omega_n^{(0)}$ denotes the surface area of the n -dimensional unit sphere. Now using (D.1), we find

$$\begin{aligned} \int d^n p (p^2 + M^2)^{-\alpha} &= \int_{-\infty}^{\infty} dp_o (-1)^\alpha C_{n-2,\alpha} (-p_o^2 - M^2)^{-\alpha + \frac{n-1}{2}} \Omega_{n-2}^{(0)} \\ &= 2(-1)^{\frac{n-1}{2}} C_{n-2,\alpha} C_{0,\alpha - \frac{n-1}{2}} \Omega_{n-2}^{(0)} M^{-2\alpha+n}. \end{aligned} \quad (\text{D.5})$$

From (D.5), it is straight forward to compute

$$\begin{aligned} \int d^n p \left(p^2 + 2p \cdot Q + M^2 \right)^{-\alpha} &= \int d^n p \left[(p+Q)^2 + M^2 - Q^2 \right]^{-\alpha} \\ &= 2(-1)^{\frac{n-1}{2}} C_{n-2,\alpha} C_{0,\alpha-\frac{n-1}{2}} \Omega_{n-2}^{(0)} \left(M^2 - Q^2 \right)^{-\alpha+\frac{n}{2}}. \end{aligned} \quad (\text{D.6})$$

Now we can also evaluate

$$\begin{aligned} \int d^n p p_\mu \left(p^2 + 2p \cdot Q + M^2 \right)^{-\alpha} &= \frac{-1}{2(\alpha-1)} \frac{\partial}{\partial Q^\mu} \int d^n p \left(p^2 + 2p \cdot Q + M^2 \right)^{-\alpha+1} \\ &= (-1)^{\frac{n+1}{2}} \frac{2(\alpha-1-\frac{n}{2})}{\alpha-1} C_{n-2,\alpha-1} \\ &\quad \times C_{0,\alpha-\frac{n+1}{2}} \Omega_{n-2}^{(0)} \left(M^2 - Q^2 \right)^{-\alpha+\frac{n}{2}} Q_\mu. \end{aligned} \quad (\text{D.7})$$

Using similar techniques we can evaluate

$$\begin{aligned} \int d^n p p_\mu p_\nu \left(p^2 + 2p \cdot Q + M^2 \right)^{-\alpha} &= (-1)^{\frac{n+3}{2}} \left(\alpha - 2 - \frac{n}{2} \right) (\alpha-1)^{-1} (\alpha-2)^{-1} \\ &\quad \times C_{n-2,\alpha-2} C_{0,\alpha-\frac{n+3}{2}} \Omega_{n-2}^{(0)} \left(M^2 - Q^2 \right)^{-\alpha+1+\frac{n}{2}} \\ &\quad \times \left[g_{\mu\nu} + \left(M^2 - Q^2 \right)^{-1} \left(-\alpha + 1 + \frac{n}{2} \right) \right. \\ &\quad \left. \times (-2Q_\mu Q_\nu) \right], \end{aligned} \quad (\text{D.8})$$

and

$$\begin{aligned} \int d^n p p^2 \left(p^2 + 2p \cdot Q + M^2 \right)^{-\alpha} &= (-1)^{\frac{n+3}{2}} \left(\alpha - 2 - \frac{n}{2} \right) (\alpha-1)^{-1} (\alpha-2)^{-1} \\ &\quad \times C_{n-2,\alpha-2} C_{0,\alpha-\frac{n+3}{2}} \Omega_{n-2}^{(0)} \left(M^2 - Q^2 \right)^{-\alpha+1+\frac{n}{2}} \\ &\quad \times \left[n + 2 \left(\alpha - 1 - \frac{n}{2} \right) \left(M^2 - Q^2 \right)^{-1} Q^2 \right], \end{aligned} \quad (\text{D.9})$$

in which $g_{\mu\nu}$ is the metric tensor

$$g_{00} = -g_{11} = -g_{22} = -g_{33} = 1, \quad (\text{D.10})$$

and all $g_{\mu\nu}$ with $\mu \neq \nu$ are 0.

We also note the following:

$$\int_0^\infty \frac{u^m}{(u^2 + M^2)^\alpha} du = \frac{-1}{\alpha - 1} \frac{\partial}{\partial M^2} \int_0^\infty \frac{u^m}{(u^2 + M^2)^{\alpha-1}} du \quad (\text{D.11})$$

Therefore, by using (D.1), we find

$$C_{m,\alpha} = \left(\alpha - 1 - \frac{m+1}{2} \right) (\alpha - 1)^{-1} C_{m,\alpha-1}. \quad (\text{D.12})$$

We can now use these results to evaluate

$$\begin{aligned} & \int d^n p_1 \left(4p_1^\mu p_1^\nu - \rho_1^2 g^{\mu\nu} \right) \left[(p_1 - Q)^2 + \rho_1^2 \right]^{-\alpha} \\ &= (-1)^{\frac{n+3}{2}} \left(\alpha - 2 - \frac{n}{2} \right) (\alpha - 1)^{-1} (\alpha - 2)^{-1} C_{n-2,\alpha-2} C_{0,\alpha-\frac{n+3}{2}} \Omega_{n-2}^{(0)} \\ & \quad \times \left[g^{\mu\nu} (4-n) (\rho_1^2 + Q^2) (\rho_1^2)^{-\alpha+\frac{n}{2}} - 4(4-n) Q^\mu Q^\nu (\rho_1^2)^{-\alpha+\frac{n}{2}} \right]. \end{aligned} \quad (\text{D.13})$$

Using (D.12) in (D.13), we find

$$\begin{aligned} & \int d^n p_1 \left(4p_1^\mu p_1^\nu - p_1^2 g^{\mu\nu} \right) \left[(p_1 - Q)^2 + \rho_1^2 \right]^{-\alpha} \\ &= (-1)^{\frac{n+3}{2}} \left(\alpha - 1 - \frac{n}{2} \right)^{-1} C_{n-2,\alpha} C_{0,\alpha-\frac{n-1}{2}} \Omega_{n-2}^{(0)} \\ & \quad \times \left[g^{\mu\nu} (4-n) (\rho_1^2 + Q^2) (\rho_1^2)^{-\alpha+\frac{n}{2}} - 4(4-n) Q^\mu Q^\nu (\rho_1^2)^{-\alpha+\frac{n}{2}} \right]. \end{aligned} \quad (\text{D.14})$$

Setting $\alpha = 3$, and taking the limit as $n \rightarrow 4$, we find

$$\begin{aligned} & \int d^n p_1 \left(4p_1^\mu p_1^\nu - p_1^2 g^{\mu\nu} \right) \left[(p_1 - Q)^2 + \rho_1^2 \right]^{-3} \\ &= (-1)^{\frac{7}{2}} \times 2\Omega_2^{(0)} \frac{1}{\rho_1^2} \left[g^{\mu\nu} (\rho_1^2 - Q^2) + 4Q^\mu Q^\nu \right] C_{2,3} C_{0,\frac{3}{2}} \\ &= -i \frac{\pi^2}{2} \frac{1}{\rho_1^2} \left[g^{\mu\nu} (\rho_1^2 - Q^2) + 4Q^\mu Q^\nu \right]. \end{aligned} \quad (\text{D.15})$$

In similar fashion we find

$$\begin{aligned} \int d^n p_1 p_1^\mu \left[(p_1 - Q)^2 + \rho_1^2 \right]^{-\alpha} &= (-1)^{\frac{n+1}{2}} 2 \left(\alpha - 1 - \frac{n}{2} \right) (\alpha - 1)^{-1} C_{n-2,\alpha-1} \\ & \quad \times C_{0,\alpha-\frac{n+1}{2}} \Omega_{n-2}^{(0)} (\rho_1^2)^{-\alpha+\frac{n}{2}} (-Q^\mu) \\ &= (-1)^{\frac{n+1}{2}} 2 C_{n-2,\alpha} C_{0,\alpha-\frac{n-1}{2}} \Omega_{n-2}^{(0)} (\rho_1^2)^{-\alpha+\frac{n}{2}} (-Q^\mu). \end{aligned} \quad (\text{D.16})$$

Therefore,

$$\begin{aligned}
 \int d^4 p_1 p_1^\mu \left[(p_1 - Q)^2 + \rho_1^2 \right]^{-3} &= -i 2 C_{2,3} C_{0, \frac{3}{2}} \Omega_2^{(0)} \frac{1}{\rho_1^2} Q^\mu \\
 &= -i \frac{\pi^2}{2} \frac{Q^\mu}{\rho_1^2}.
 \end{aligned} \tag{D.17}$$

Finally,

$$\begin{aligned}
 \int d^4 p_1 p_1^\mu \left[(p_1 - Q)^2 + \rho_1^2 \right] &= 2(-1)^{3/2} C_{2,3} C_{0, \frac{3}{2}} \Omega_2^{(0)} \frac{1}{\rho_1^2} \\
 &= -i \frac{\pi^2}{2} \frac{1}{\rho_1^2}.
 \end{aligned} \tag{D.18}$$

Appendix E. Stopping Power

Consider the reaction



in which X represents one or more particles produced in the process. Let Z_1 be an incident particle, and Z_2 represent a fixed target, whose density is ρ (number of nuclei per unit volume). Let σ denote the cross section for the process (E.1), and E_x the energy of the system X . If we disregard the effect due to recoil of Z_2 , then by the conservation of energy, the energy loss of Z_1 is equal to E_x . Consider a slab of the target Z_2 of cross-sectional area A and thickness Δx .

Figure E.1

The number of Z_2 nuclei in this slab is $\rho A \Delta x$. The cross section for an incident particle Z_1 to collide with a Z_2 , producing X is given by

$$\Delta\sigma = \rho A \Delta x \frac{d\sigma}{dE_x} dE_x, \quad (\text{E.2})$$

where we assume the energy of the produced system X to be between E_x and $E_x + dE_x$.

Therefore the probability for this process is

$$P(E_x)dE_x = \frac{\Delta\sigma}{A} = \rho\Delta x \frac{d\sigma}{dE_x} dE_x, \quad (\text{E.3})$$

in which $P(E_x)$ represents the probability density for the process. Therefore the total energy loss by the incident particle Z_1 per unit length is given by

$$-\frac{dE}{dx} = \lim_{\Delta x \rightarrow 0} \frac{1}{\Delta x} \int E_x P(E_x) dE_x \quad (\text{E.4a})$$

$$= \rho \int E_x \frac{d\sigma}{dE_x} dE_x. \quad (\text{E.4b})$$

The $-$ sign in (E.4) signifies the fact that energy is lost by Z_1 in the process, so that the change in its energy dE is negative. See ref. 16, eq (6.4), page 741.

For two-photon processes of the kind that we have considered

$$E_x = \omega_1 + \omega_2, \quad (\text{E.5})$$

in which again we use the “natural units” for which $\hbar = 1$. The cross section is given by (2.2a). By switching the variables of integration from ω_1, ω_2 to ω_1, E_x , and using the fact

$$d\omega_1 d\omega_2 = d\omega_1 dE_x, \quad (\text{E.6})$$

which can be obtained from (E.5), (E.4b) can be written in the form

$$-\frac{dE}{dx} = \rho \int \frac{d\omega_1}{\omega_1} \int \frac{dE_x}{E_x - \omega_1} E_x F(\omega_1, E_x - \omega_1) \times \sigma_{\gamma\gamma}(\omega_1, E_x - \omega_1) \quad (\text{E.7a})$$

$$= \rho \int \frac{d\omega_1}{\omega_1} \int \frac{d\omega_2}{\omega_2} (\omega_1 + \omega_2) F(\omega_1, \omega_2) \sigma_{\gamma\gamma}(\omega_1, \omega_2) \quad (\text{E.7b})$$

(E.7b) is the same as (2.7).

References

1. Fatyga, M.; and Norbury, J. W.: An Experiment to Study Strong Electromagnetic Fields at RHIC. Proceedings of the Fourth Workshop on Experiments and Detectors for a Relativistic Heavy Ion Collider, Brookhaven National Laboratory, July 1990, pp. 345–368.
2. Papageorgiu, E.: Two-photon Physics With Ultra-High-Energy Heavy-Ion Beams. *Phys. Lett. B*, vol. 250, no. 1,2, Nov. 1990, pp. 155–160.
3. Baur, G.; and Ferreira Filho, L. G.: Coherent Particle Production at Relativistic Heavy-ion Colliders Including Strong Absorption Effects. *Nucl. Phys. A*, vol. 518, 1990, pp. 786–800.
4. Jackson, J. D.: *Classical Electrodynamics*, John Wiley & Sons, Inc., 1975.
5. Budnev, V. M.; Ginzburg, I. F.; Meledin, G. V.; and Serbo, V. G.: The Two-Photon Particle Production Mechanism. *Physical Problems. Applications. Equivalent Photon Approximation. Phys. Rep.*, vol. 15, 1975, pp. 181–282.
6. Vermaseren, J. A. M.: Two-Photon Processes at Very High Energies. *Nucl. Phys. B*, vol. 229, 1983, pp. 347–371.
7. Bottcher, C.; and Strayer, M. R.: Electron Pair Production From Pulsed Electromagnetic Fields in Relativistic Heavy-Ion Collisions. *Phys. Rev. D*, vol. 39, no. 5, March 1989, pp. 1330–1341.
8. Wu, J. S.; Bottcher, C.; and Strayer, M. R.: Coherent Particle Production in a Classical Field Approximation. *Phys. Lett. B*, vol. 252, no. 1, Dec. 1990, pp. 37–42.
9. Commins, E. D.: *Weak Interactions*. McGraw Hill, Inc., 1973.
10. Wilson, John W. et al.: *Transport Methods and Interactions for Space Radiations*. NASA Reference Publication 1257, December 1991.
11. Rhoades-Brown, M. J.; and Weneser, J.: Higher Order Effects on Pair Creation by Relativistic Heavy Ion Beams. *Phys. Rev. A*, vol. 44, no. 1, July 1991, pp. 330–336.
12. Bertulani, C. A.; and Baur, G.: Electromagnetic Processes in Relativistic Heavy Ion Collisions. *Phys. Rep.*, vol. 163, nos. 5 & 6, June 1988, pp. 299–408.

13. Papageorgiu, E.: Coherent Higgs-Bosons Production in Relativistic Heavy-Ion Collisions. *Phys. Rev. D*, vol. 40, no. 1, July 1989, pp. 92–100.
14. Lee, T. D.: *Particle Physics and Introduction to Field Theory*. Harwood Academic Publishers, 1981.
15. Frampton, P. H.: *Gauge Field Theories*. The Benjamin/Cummings Publishing Company, Inc., 1987.
16. Bertulani, C. A.; and Baur, G.: Electromagnetic Processes in Relativistic Heavy Ion Collisions. *Nucl. Phys. A*, vol. 458, 1986, pp. 725–744.

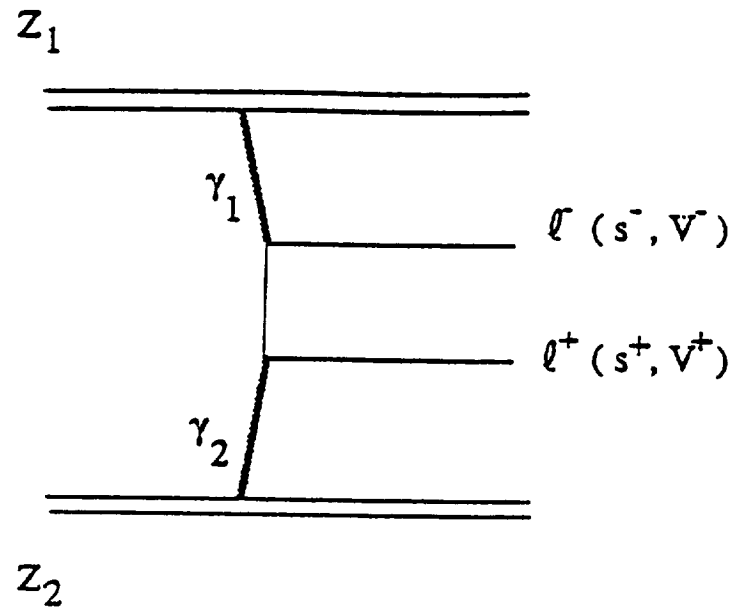


Figure 1. A Feynman diagram for the processes $Z_1 Z_2 \rightarrow Z_1 Z_2 \ell^+ \ell^-$, $Z_1 Z_2 \rightarrow Z_1 Z_2 s^+ s^-$, and $Z_1 Z_2 \rightarrow Z_1 Z_2 V^+ V^-$.

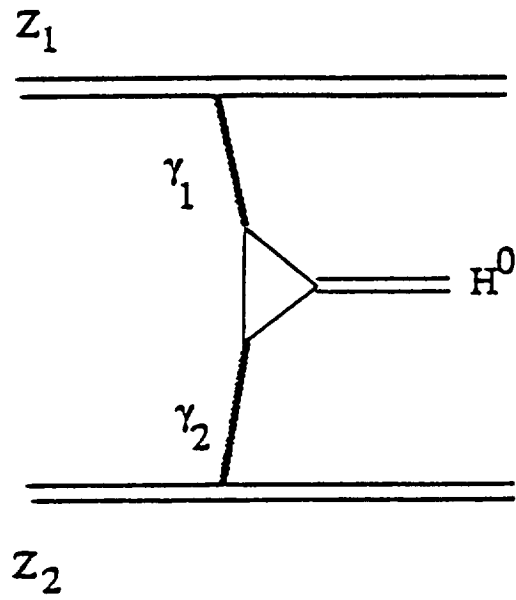


Figure 2. A Feynman diagram for the process $Z_1 Z_2 \rightarrow Z_1 Z_2 H^0$.

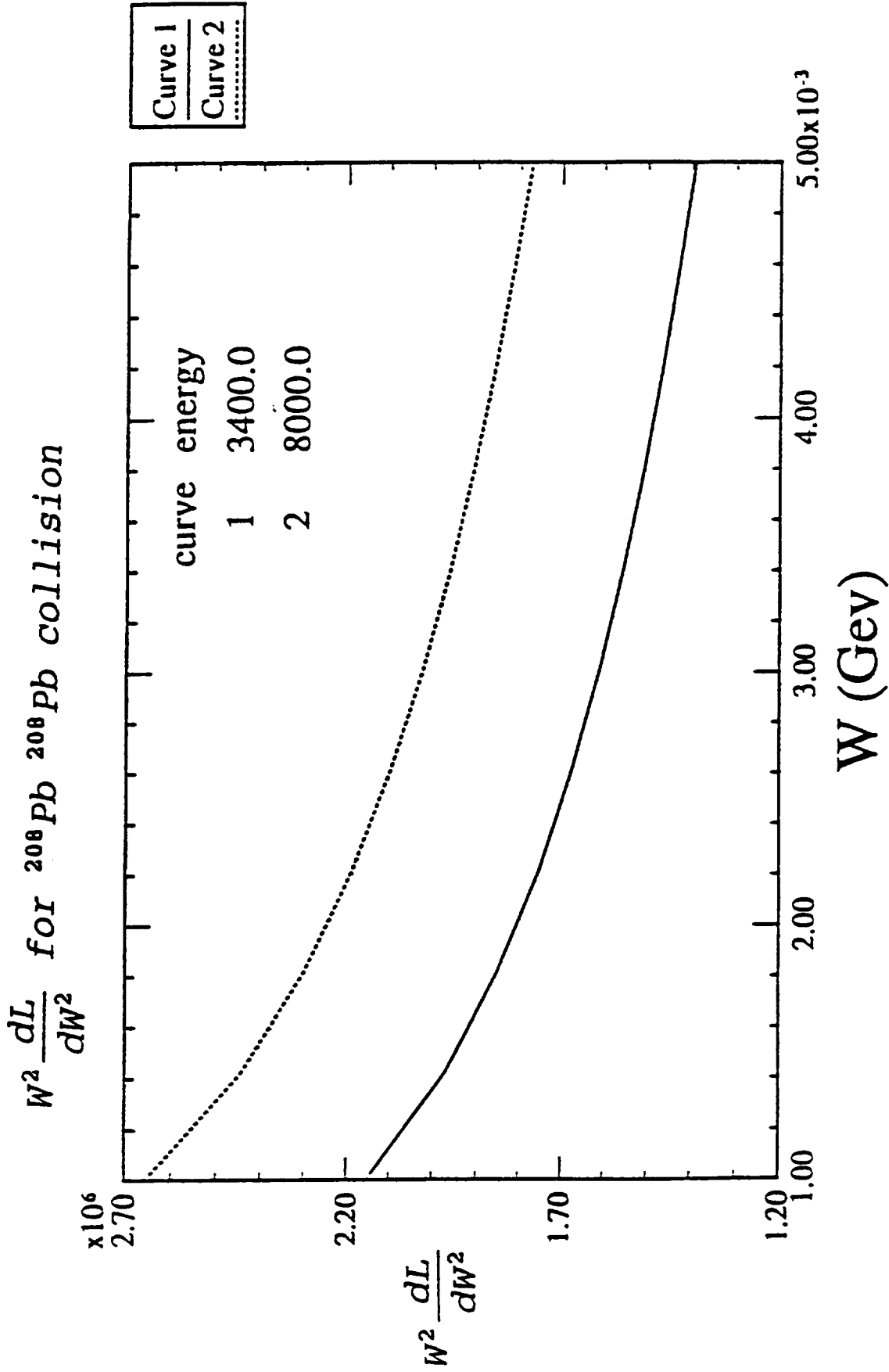


Figure 3. Plots of $W^2 \frac{dL}{dW^2}$.

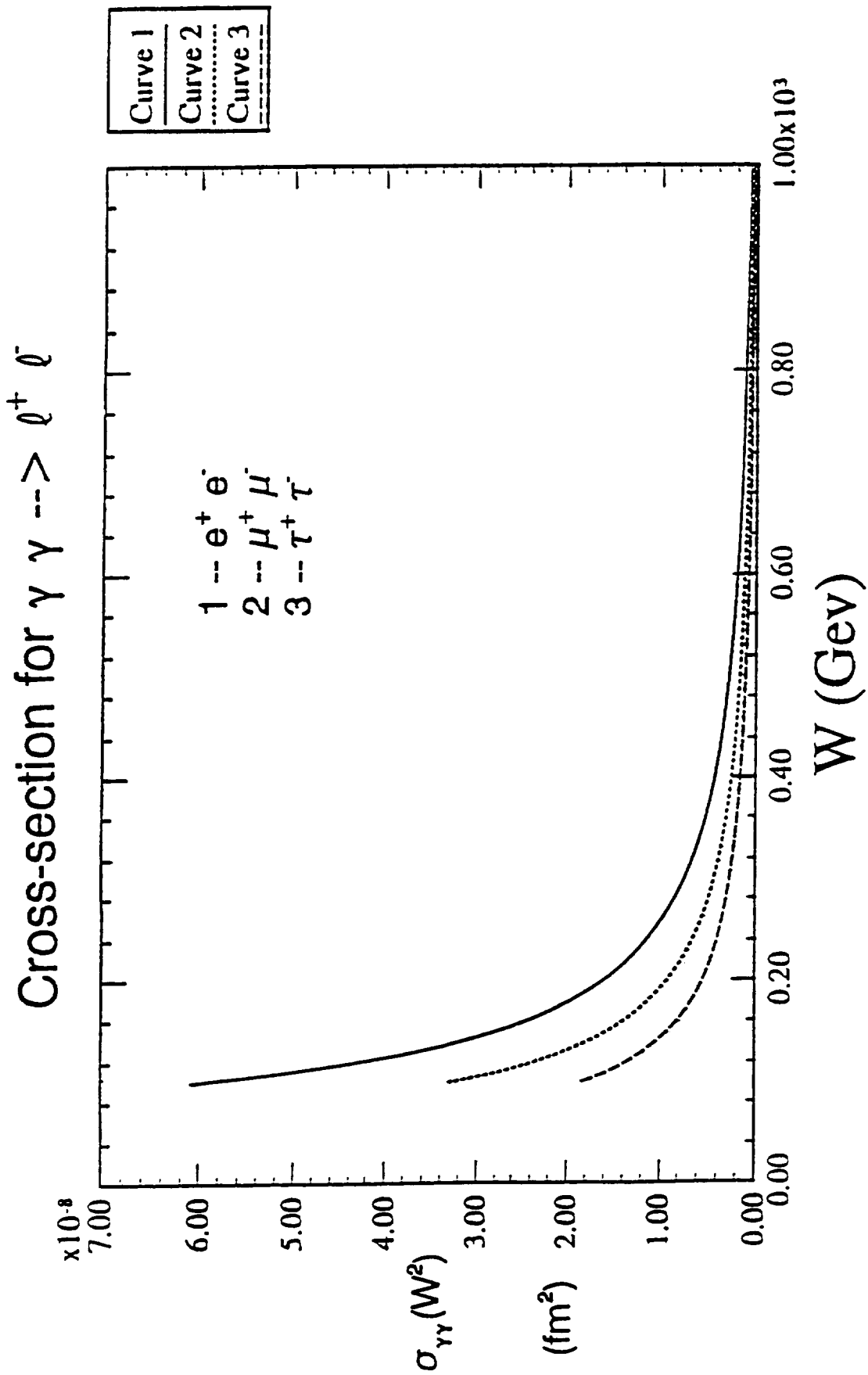


Figure 4a. $\sigma_{\gamma\gamma}(W^2)$ for the reaction $\gamma\gamma \rightarrow \ell^+ \ell^-$.

Cross-section for $\gamma \gamma \rightarrow s^+ s^-$

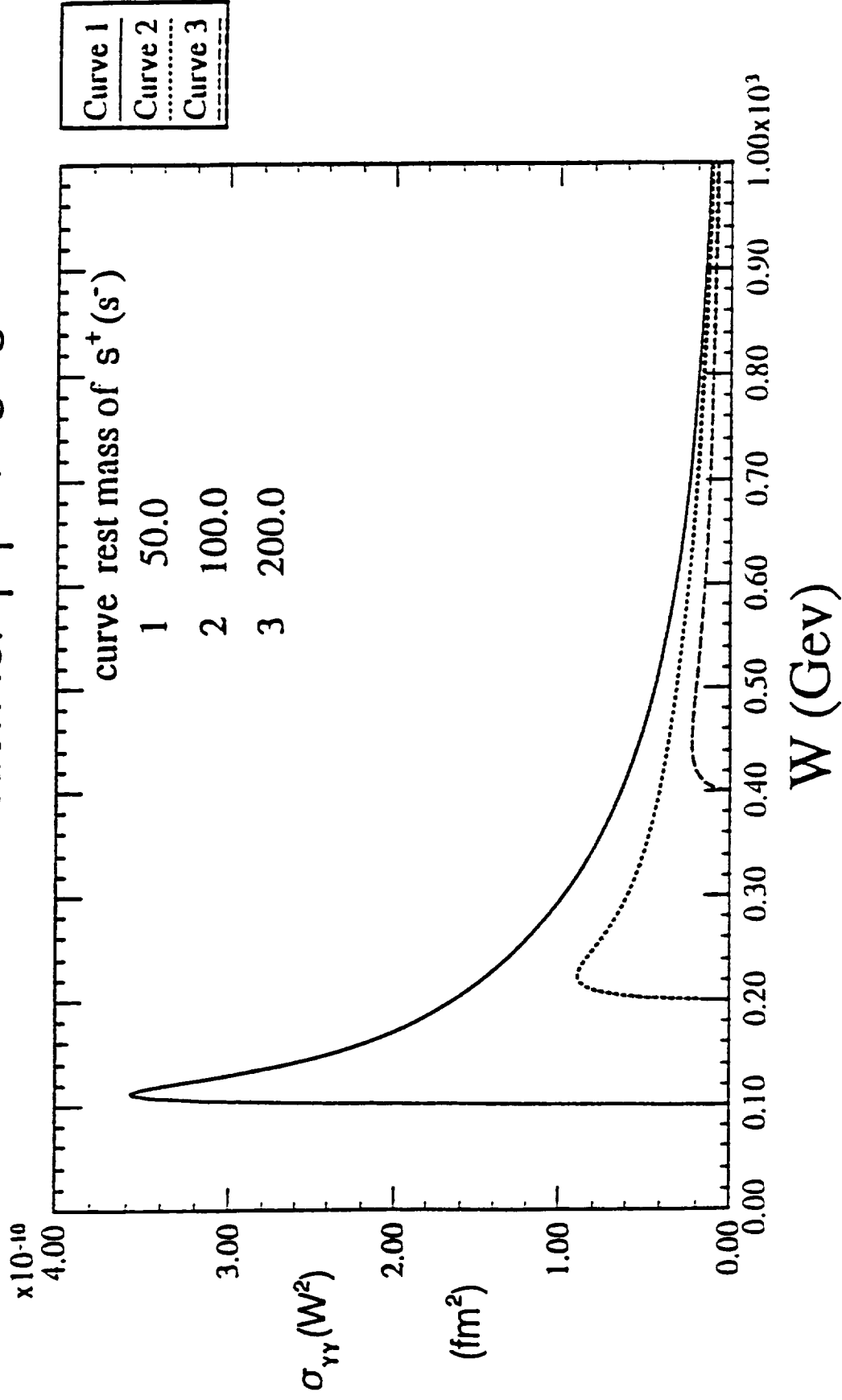


Figure 4b. $\sigma_{\gamma\gamma}(W^2)$ for the reaction $\gamma\gamma \rightarrow s^+ s^-$.

Cross-section for $\gamma \gamma \rightarrow V^+ V^-$

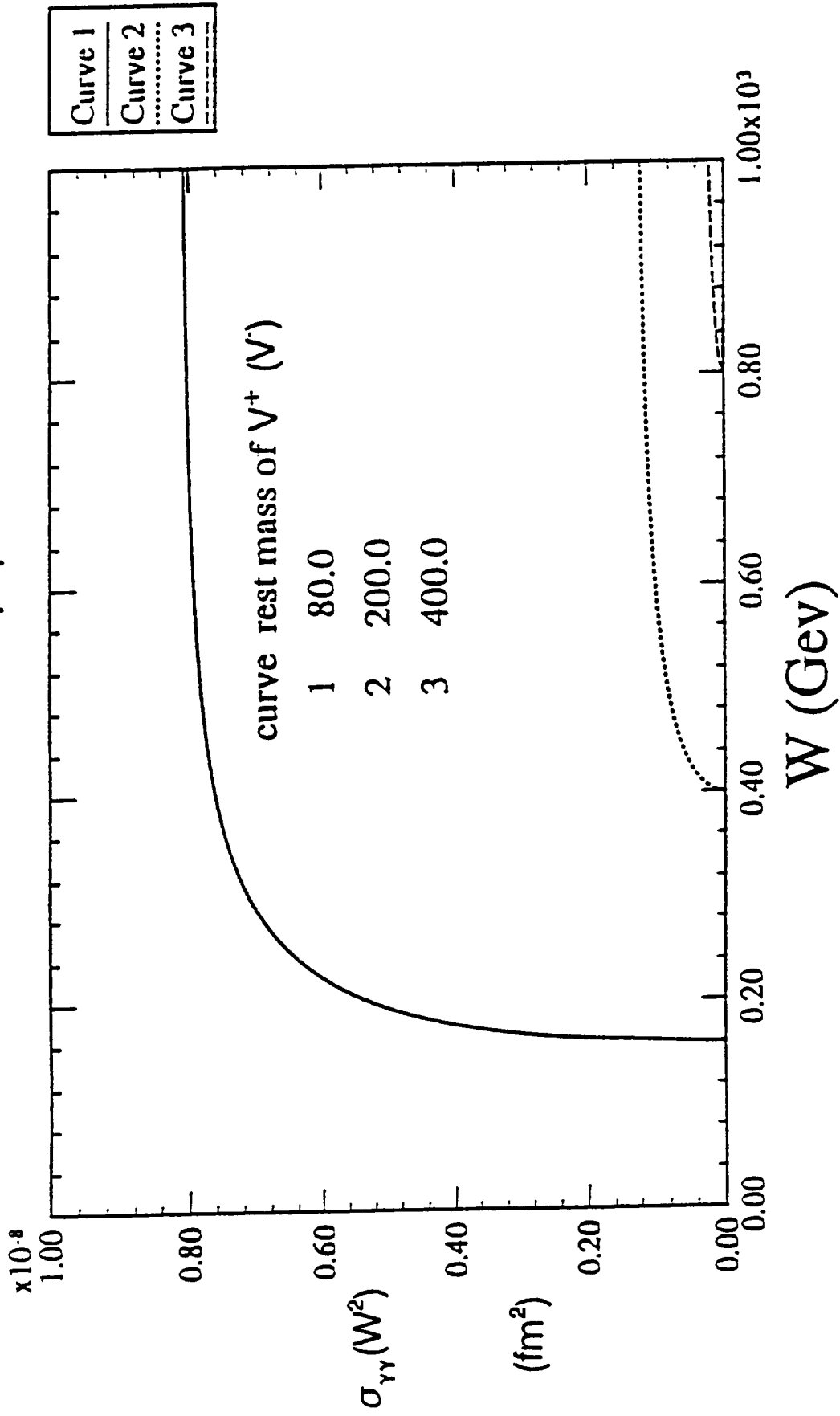


Figure 4c. $\sigma_{\gamma\gamma}(W^2)$ for the reaction $\gamma\gamma \rightarrow V^+ V^-$.

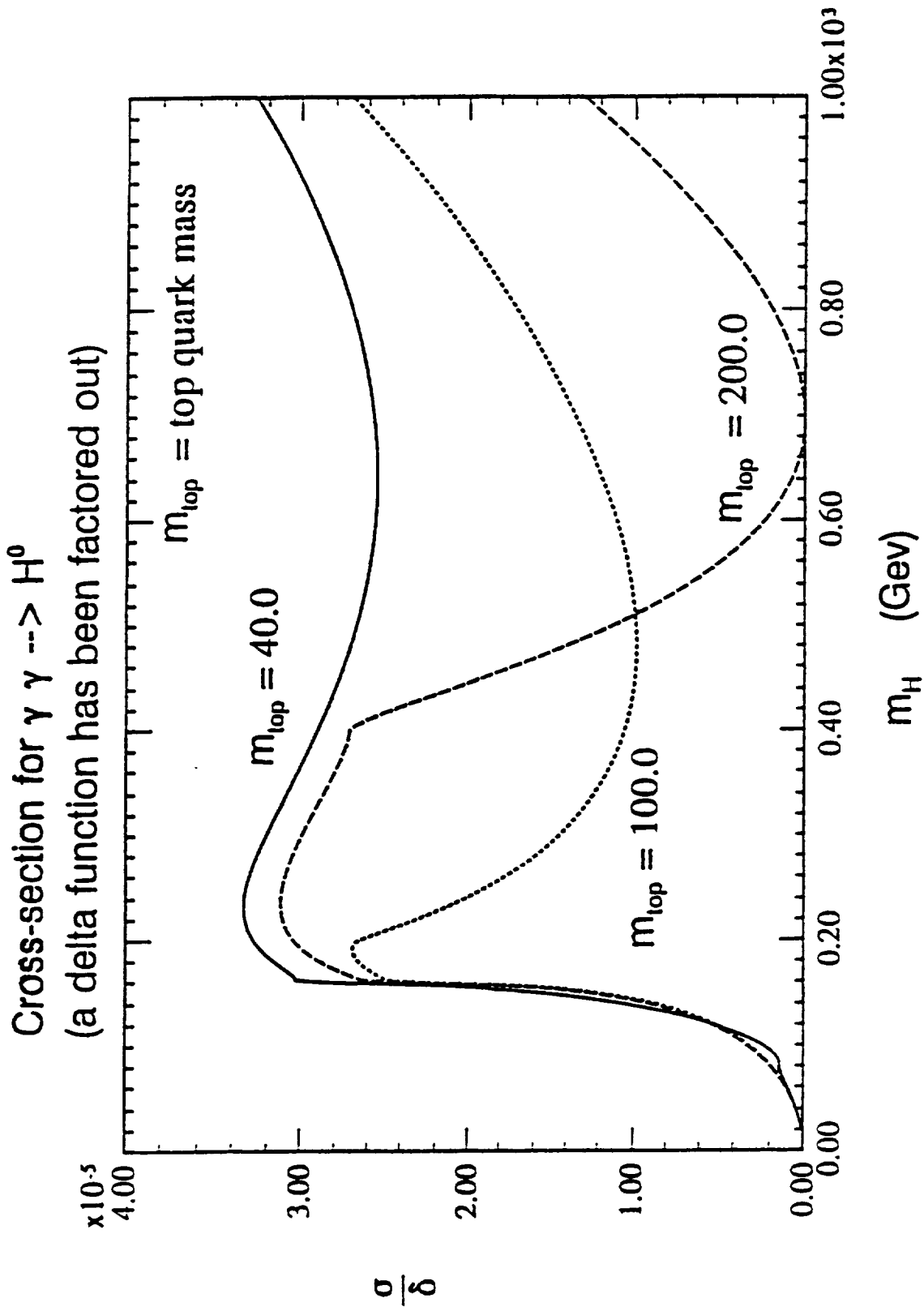


Figure 4d. $\sigma_{\gamma\gamma}(W^2)$ for the reaction $\gamma\gamma \rightarrow H^0$.

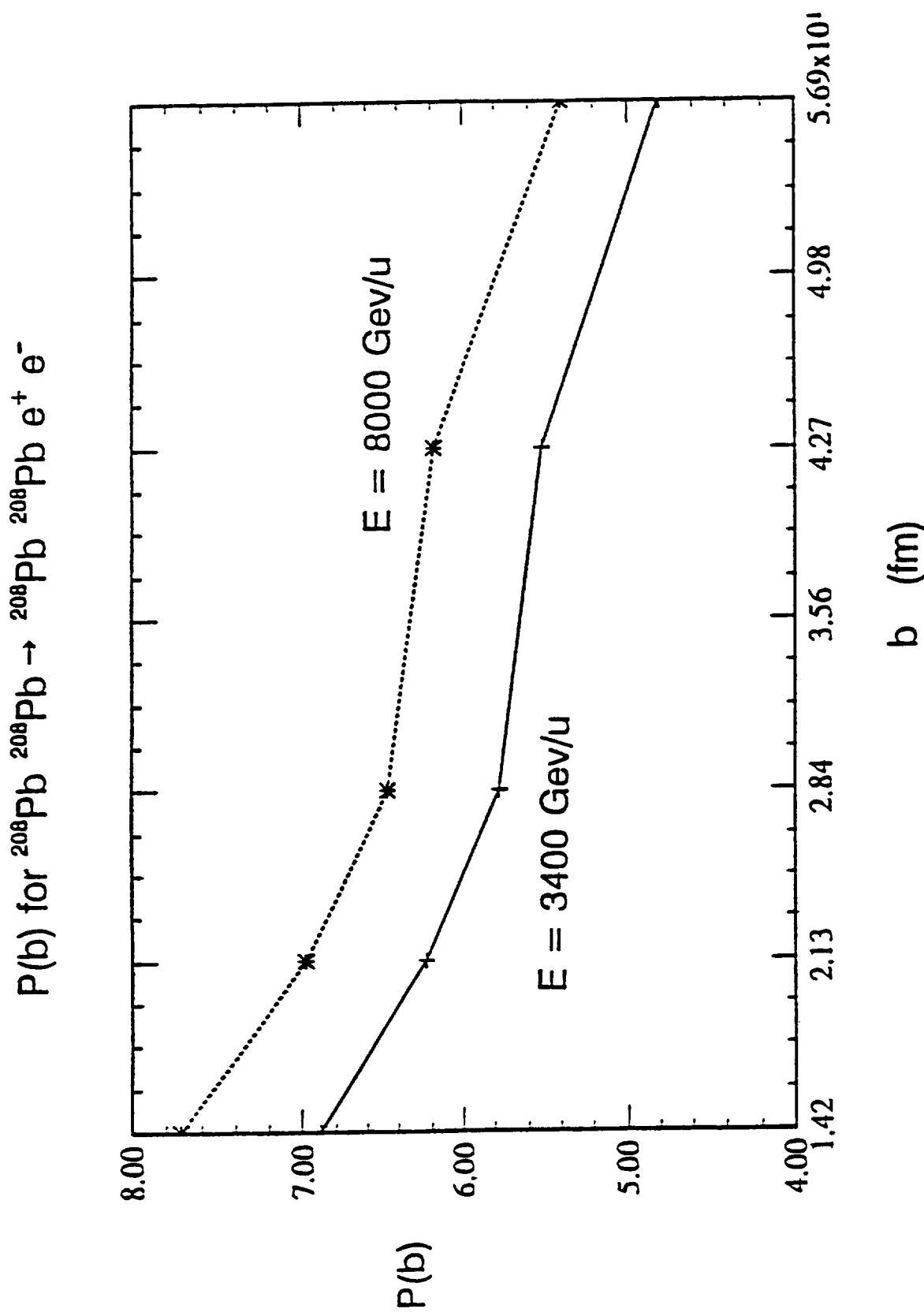


Figure 5. Plots of $P(b)$ for the reaction $^{208}\text{Pb } ^{208}\text{Pb} \rightarrow ^{208}\text{Pb } ^{208}\text{Pb } e^+ e^-$ at different energies.
 Note: These plots are only rough estimates.

Cross-section for $^{208}\text{Pb } ^{208}\text{Pb} \rightarrow ^{208}\text{Pb } ^{208}\text{Pb } H^0$

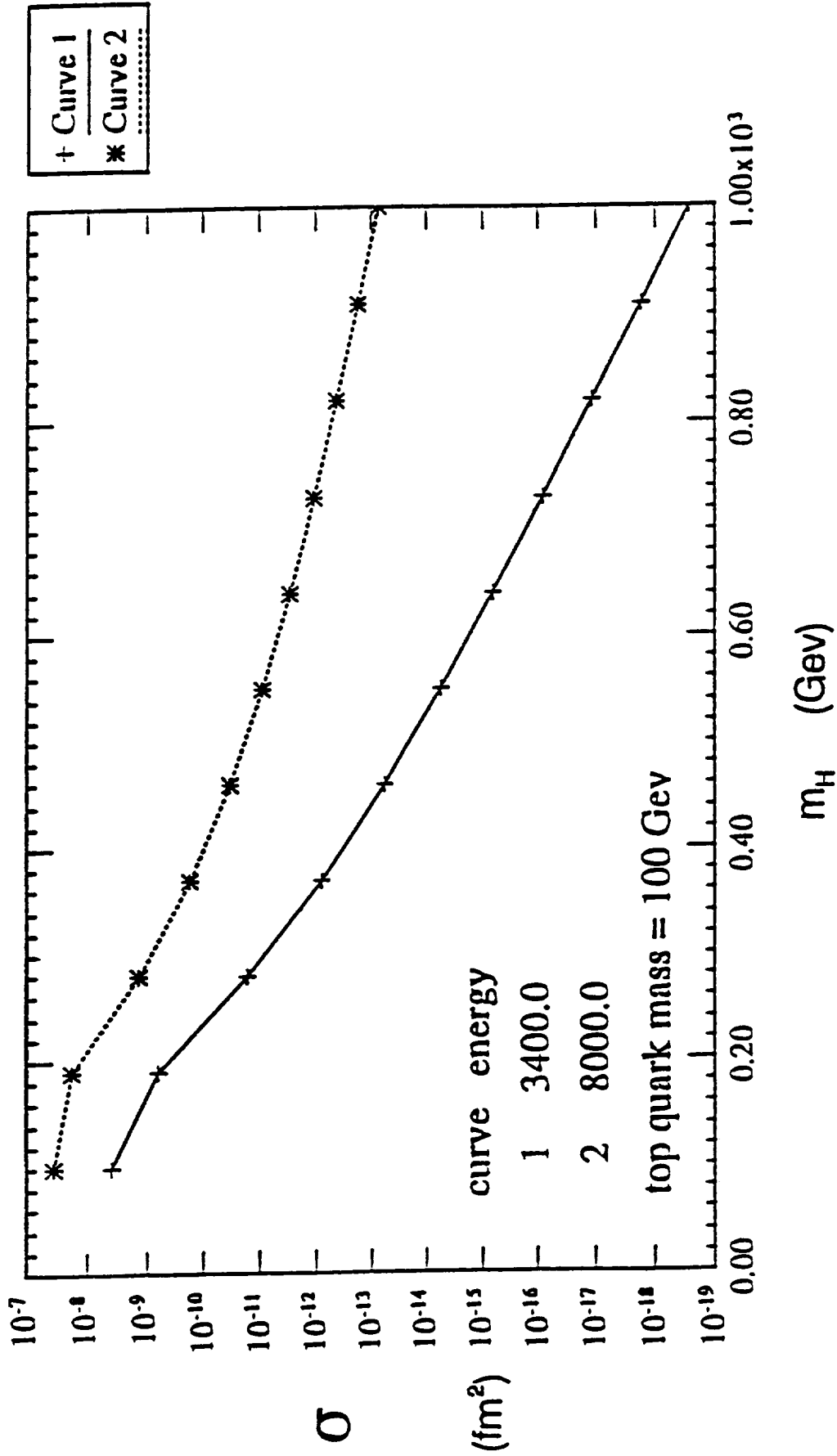


Figure 6. Plots of the total cross section for the process $^{208}\text{Pb } ^{208}\text{Pb} \rightarrow ^{208}\text{Pb } ^{208}\text{Pb } H^0$.

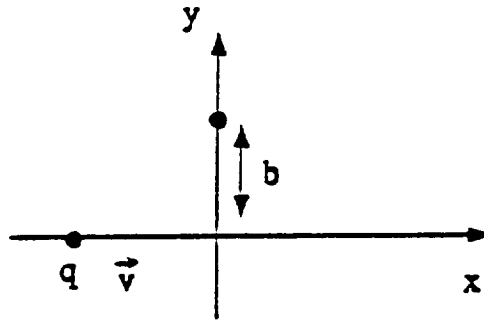


Figure A.1. Electromagnetic fields generated by a charge q moving along the x -axis.

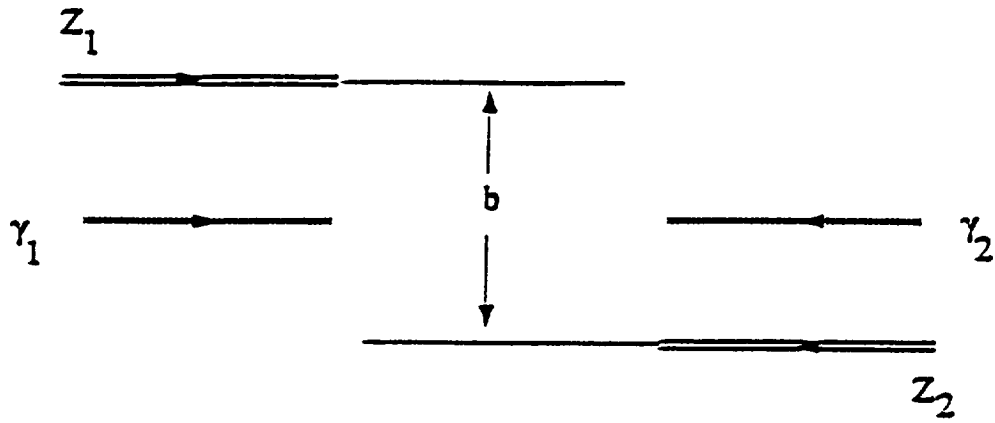


Figure A.2. Photons emitted by two colliding nuclei, viewed along the direction of motion of the nuclei in their center of momentum frame.

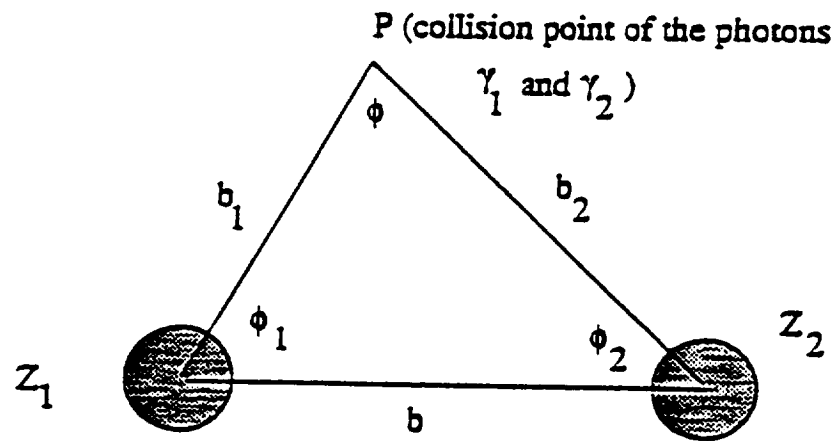


Figure A.3. Cross-sectional view of the collision of two nuclei.

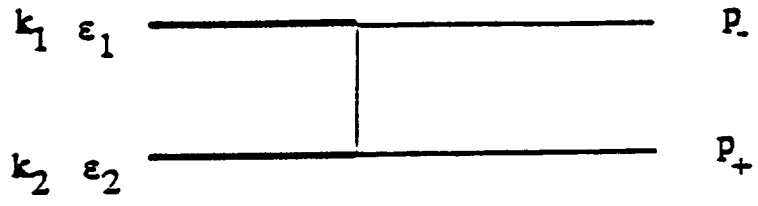


Figure B.1a

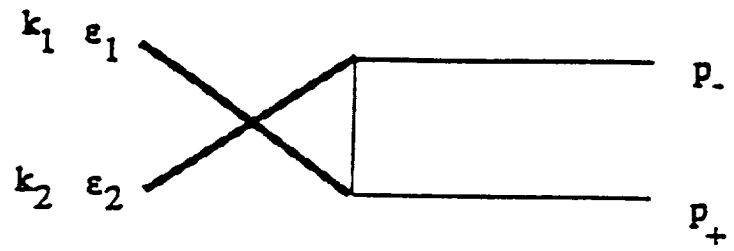


Figure B.1b

Figure B.1a-b. Second order Feynman diagrams for the process $\gamma\gamma \rightarrow s^+s^-$.

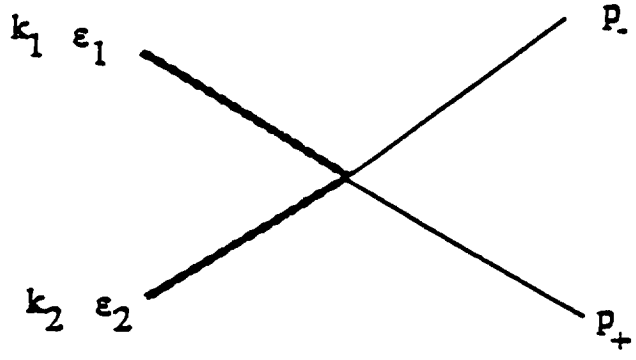


Figure B.2: First order Feynman diagram for the process $\gamma\gamma \rightarrow s^+s^-$.

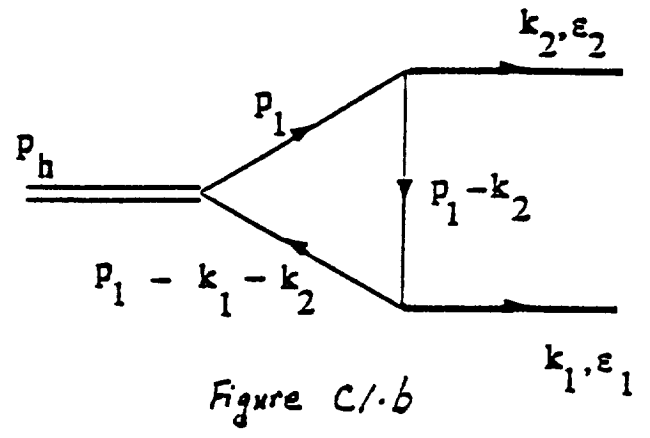
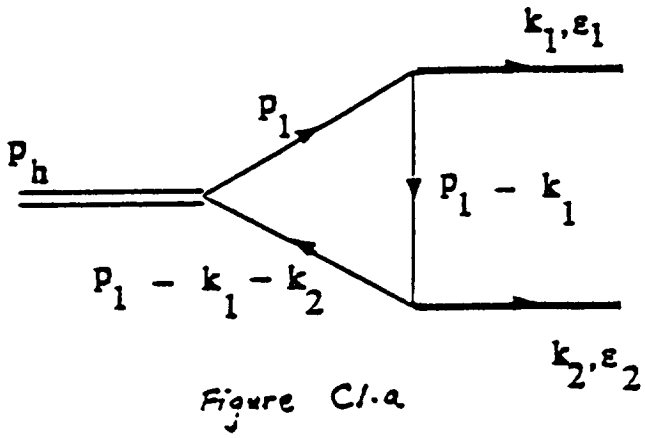


Figure C.1a-b. Feynman diagrams representing fermion contribution to the process $H^0 \rightarrow \gamma\gamma$.

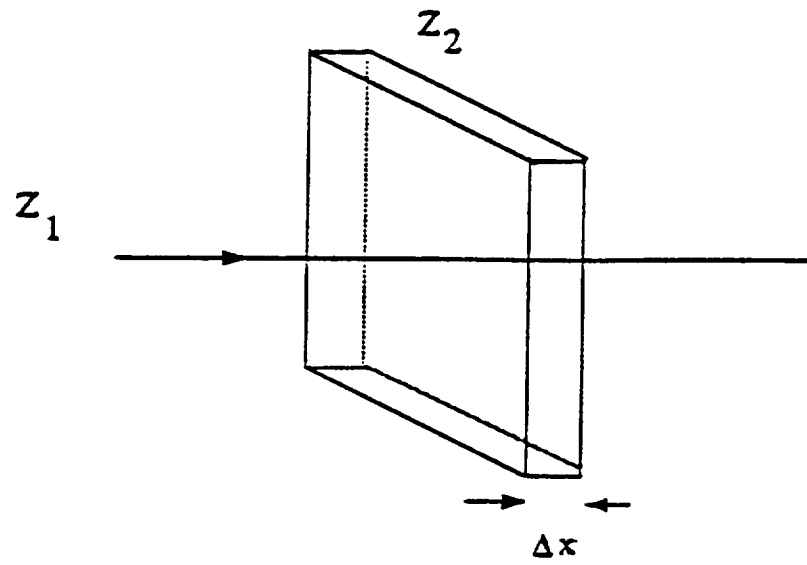


Figure E.1: A beam of particles Z_1 incident on a fixed target Z_2 .

REPORT DOCUMENTATION PAGE

Form Approved
OMB No. 0704-0188

Public reporting burden for this collection of information is estimated to average 1 hour per response, including the time for reviewing instructions, searching existing data sources, gathering and maintaining the data needed, and completing and reviewing the collection of information. Send comments regarding this burden estimate or any other aspect of this collection of information, including suggestions for reducing this burden, to Washington Headquarters Services, Directorate for Information Operations and Reports, 1215 Jefferson Davis Highway, Suite 1204, Arlington, VA 22202-4302, and to the Office of Management and Budget, Paperwork Reduction Project (0704-0188), Washington, DC 20503.

1. AGENCY USE ONLY (Leave blank)	2. REPORT DATE March 1994	3. REPORT TYPE AND DATES COVERED Contractor Report
---	-------------------------------------	--

4. TITLE AND SUBTITLE Stopping Powers and Cross Sections Due to Two-Photon Processes in Relativistic Nucleus-Nucleus Collisions	5. FUNDING NUMBERS G NAG1-1457 WU 199-45-16-11
6. AUTHOR(S) Wang K. Cheung John W. Norbury	

7. PERFORMING ORGANIZATION NAME(S) AND ADDRESS(ES) Physics Department University of Wisconsin La Crosse, WI 54601	8. PERFORMING ORGANIZATION REPORT NUMBER
---	---

9. SPONSORING/MONITORING AGENCY NAME(S) AND ADDRESS(ES) National Aeronautics and Space Administration Langley Research Center Hampton, VA 23681-0001	10. SPONSORING/MONITORING AGENCY REPORT NUMBER NASA CR-4574
--	---

11. SUPPLEMENTARY NOTES
Langley Technical Monitor: Francis A. Cucinotta
Final Report

12a. DISTRIBUTION/AVAILABILITY STATEMENT Unclassified--Unlimited Subject Category 73	12b. DISTRIBUTION CODE
---	-------------------------------

13. ABSTRACT (Maximum 200 words)
The effects of electromagnetic-production processes due to two-photon exchange in nucleus-nucleus collisions are discussed. Feynman diagrams for two-photon exchange are evaluated using quantum electrodynamics. The total cross section and stopping power for projectile and target nuclei of identical charge are found to be significant for heavy nuclei above a few GeV per nucleon-incident energy.

14. SUBJECT TERMS Nucleus-nucleus collisions; Galactic cosmic rays; Two-photon collisions; Stopping power	15. NUMBER OF PAGES 60
	16. PRICE CODE A04

17. SECURITY CLASSIFICATION OF REPORT Unclassified	18. SECURITY CLASSIFICATION OF THIS PAGE Unclassified	19. SECURITY CLASSIFICATION OF ABSTRACT	20. LIMITATION OF ABSTRACT
--	---	--	-----------------------------------